TÉCNICO LISBOA

Geostatistical History Matching with Seismic Data Integration

Jorge Miguel Fernandes de Oliveira

Thesis to obtain the Master of Science Degree in

Petroleum Engineering

Supervisor: Professor Doutor Leonardo Azevedo Guerra Raposo Pereira

Examination Committee

Chairperson: Profª Doutora Maria João Correia Colunas Pereira

Supervisor: Prof Doutor Leonardo Azevedo Guerra Raposo Pereira

Members of the Committee: Prof Doutor Amílcar de Oliveira Soares

November, 2016

Acknowledgements

I would like to express my deepest gratitude to my supervisor Doctor Leonardo Azevedo for giving me the opportunity to develop and implement this work and for the constant support, encouragement, friendship and guidance through the difficult path and help me with many of my doubts and dilemmas, I will always have him as my reference. Thank you for always believe and for all the advices, without this teaching and motivation this thesis would not be possible.

I want to thank to CERENA for the support and working conditions as well as to providing the necessary data sets to test and implement this thesis algorithm.

I also would like to thank to IST MSc students and PhD students for making this journey easier and happier, encouraging me and being next to me in difficult moments of study, work and fun. Thank you Gonçalo 'Roze' Rodrigues, Valter Proença, Catarina Amaro, Pedro 'Minhoca' Pereira, Gonçalo Simões, Eduardo 'Prof Edu' Barrela, José Viu, Jose Campuzano, Sergio Bardera, Tipping and to one of my oldest friend Pedro Reis for always being present no matter the distance. I need to thank you to my brother from another mother, Pedro Cardoso and André Branco, for being always there for me during all my life.

Enormous thanks to my parents, João and Otelinda, and to my brother Ricardo, without them I will never had the opportunity to do this work. Thanks to my family for always being there for me, even when nothing made sense, especially to my cousins Hugo and Bruno Rações.

Dedication

To my father João memory.

Abstract

This thesis intends to address a relevant problem of the oil and gas industry related with the modelling and characterization of hydrocarbon reservoirs that honour simultaneously existing historical production data and seismic reflection data, i.e. the integration of seismic reflection data into history matching. By honouring all available data the resulting reservoir models have a better chance to predict the reservoir behaviour. The proposed geostatistical history matching with seismic data integration procedure is an iterative methodology based on a genetic algorithm, acting as a global optimizer, where the perturbation of the models parameters is performed recurring to stochastic sequential simulation and co-simulation. The proposed workflow starts with the stochastic simulation of petro-elastic models, forward modelling and the comparison against the observed seismic and production data and the simulated ones. The definition of areas of influence for each well was tackled by two different approaches. According to a geometric criteria and based on the non-linear relationship between the model parameters (permeability) and the state variables (production deviations) in terms of correlation coefficients. The selection of the conditioning data for the next iterations is based on the petro-elastic ensemble simulated at the current iteration with better response in the MDS. The results were promising according with the expectations, since the match towards the observed seismic and historic production data was achieved. The small and large scale geological patterns were reproduced in the inverted petro-elastic models even when the reservoir model is perturbed in all its extension.

Keywords: History Matching, Geostatistical modelling, seismic data integration, reservoir characterization.

Resumo

A presente tese pretende abordar um problema relevante na indústria relacionado com a modelação e caracterização de reservatórios petrolíferos, a integração de dados de reflexão sísmica no processo de ajuste histórico, em que o histórico de produção e a sísmica sejam simultaneamente honrados. Ao honrarem todos os dados disponíveis, os modelos de reservatório resultantes têm uma maior capacidade de prever o comportamento do reservatório. O procedimento proposto, *history matching* geostatístico com integração de dados sísmicos, é uma metodologia iterativa baseada num algoritmo genético que actua como optimizador global, em que a perturbação dos parâmetros do modelo é feita recorrendo à simulação sequencial estocástica e co-simulação. A estrutura proposta tem início com a simulação estocástica de modelos petro-elásticos, modelação direta e comparação da sísmica e o histórico de produção observados com os simulados. A definição de áreas de influência de cada poço foi definida mediante duas abordagens. De acordo com um critério geométrico e baseado na relação não-linear entre os parâmetros do modelo (permeabilidade) e as variáveis dinâmicas (desvios de produção) sob a forma de coeficientes de correlação. A seleção de dados condicionantes para as seguintes iterações baseia-se no conjunto de dados simulados com melhor resposta no espaço MDS após cada iteração. Os resultados foram promissores, tendo em conta as expectativas, uma vez que a similitude perante os dados sísmicos e de histórico de produção foi alcançada. As características geológicas de menor e maior escala foram reproduzidas nos modelos petro-elásticos invertidos, mesmo quando é perturbado em toda a sua extensão.

Palavras-chave: *History matching*; modelação geostatística; integração de dados sísmicos; caracterização do reservatório, MDS, simulação sequencial e co-simulação.

Contents

List of Figures

List of Tables

Chapter 1. Introduction

1.1. Scope of the problem

The economic viability of oilfield development projects is greatly influenced by the reservoir's performance under the current and future operation conditions (Rwechungura et al. 2011). To achieve an efficient reservoir management process it is essential to evaluate the past and present reservoir performance for forecast its future. In 2003 the IEA (International Energy Agency) forecasted that the oil and gas business will spend around 4 trillion dollars in the next 20 years to simply maintain the production at the current levels (Hajizadeh et al. 2010). Nowadays, one of the company's goals to make projects more profitable is the development of new tools which aims to accurately estimate and predict the future performance of hydrocarbon reservoirs. New techniques able to integrate all available data during the reservoir modelling stage is the correct answer to face these new challenges.

The reservoir modelling should represent, in a reliable way, the reservoir characteristics as long as the understating about the geology of the reservoir and its petrophysical evolves, which lies on the integration of all available data into a three-dimensional model in order to describe the spatial distribution of the internal petrophysical properties (e.g. porosity and permeability) and infer about the subsurface fluid flow patterns (e.g. oil and water). However, this is by far not a trivial task since input data (both static and dynamic) are collected under extreme conditions which may lead to substantial uncertainty in the measurements and interpretation of the data. The available data is mostly discrete, sparse and with different support volume and resolution, such as well logs and seismic surveys, and in a later stage, while the reservoir starts producing, the historic production data. Thus, if the reservoir model should be used as input to key reservoir management decisions, it is very important that the uncertainty both in terms of the data measurements and their associated interpretation be quantified and captured. This uncertainty is not homogeneously distributed along the entire reservoir: is lower in areas near wells locations and higher in areas far from those; which concerns to the lack of knowledge related to the physical processes that is intended to model and the complexity of the natural phenomena. Hence, stochastic approach is a natural solution of the reservoir modelling problem. By assessing the uncertainty of these models it is possible to decrease the risk level and consequently costs related with a given hydrocarbon reservoir, allowing better management decisions, such as the definition of the number and the location of new wells, the amount of existing oil and predict the economic return generated by the same (Caers 2011; Azevedo 2013).

The initial petrophysical model characterized from well-logs and seismic surveys, usually labelled as static model, may not be enough to estimate and model information such as oil original in place and to predict the behavior of the reservoir during production and since its relationship with the fluid production is highly non-linear. To understand the complex nature and behavior of hydrocarbon reservoir during production it is used the reservoir fluid flow simulation, typically in the form of fluid rate and pressure data. When it comes to the integration of dynamic data, also known as history matching, the key modelling uncertainties captured and quantified in the static data conditioning recurring to geostatistical

tools may have been lost in the history matching phase since this process is usually performed by modifying the geological reservoir properties (static model) to match the observed historic production data. In other words, the history matching aims to calibrate the model of the internal reservoir's properties of interest, such as porosity and permeability, by perturbing the parameter model space until the match between simulated and observed historic production data through the use of simple or combined objective function is reached (Mata-Lima 2008). However, this is an ill-posed problem, nonlinear and with non-unique solution where different models can match the observed production data. The consistency between the input data and the resulting reservoir model is usually lost in traditional history matching. Thus, it is not surprising that the predictability of these reservoir models are often very poor. The key to improved reservoir model predictions is therefore to quantify and capture the modelling uncertainties by consistently integrating both static and dynamic data measurement (Hoffman 2005; Caeiro 2014).

Different authors studied this problem and proposed alternative solutions to improve it. Initially approached in the 60's by the adjustment of reservoir parameters to the pressure data, Kruger (1960) and after Chen (1973) introduced a popular method, the optimal control theory for obtaining history matched models. However, the modern era of history matching only started in the 90's, by the introduction of simulated annealing techniques, as global optimization algorithm (Ouenes et al. 1994), and by the recognition of the importance to assess the uncertainty by examining multiple models (Tyler 1993). Recently, the main approaches to solve the history matching problems are: (i) data assimilation methods, (ii) stochastic optimization methods and (iii) perturbation methods. Data assimilation methods gradually assimilate an ensemble of models to the sequence of dynamic observations using updating of the ensemble, such as Ensemble Kalman Filters (EnKF; Evensen et al. 2007). Neighbourhood algorithm (NA; Sambridge 1999), Genetic algorithms (GA; Erbas et al. 2007), Particle Swarm Optimization (PSO; Mohamed et al. 2010) and Differential Evolution (DE; Hajizadeh et al. 2010) are some of the stochastic methods which are able to find multiple local minima assuming that a global minima cannot be differentiated. Gradual deformation (Roggero et al. 1998; Hu et al. 2001), Probability perturbation (Caers and Hoffman 2006) and Co-simulation (Mata-Lima 2008; Le Ravalec-Dupin 2011) are an example of the perturbation methods that according to a slack parameter perturb the model regionally. However, these methods have difficulties when applied to non-stationary geological environments, such as turbidites.

The convergence of non-stationary models, such as channelized deltaic structures, due to the heterogeneous distribution of the reservoir properties is very difficult because small changes in the channels shape can cause large changes in the simulated production data, particularly evident as spatial connectivity of the channels (Caeiro 2014). Variogram-based stochastic algorithms are hardly suitable to model conveniently sedimentary environments associated with channelized systems and its high variability in terms of shape and thickness of the many meandering channels. The perturbation and the stochastic optimization methods when applied to these reservoirs show difficulties in accurately characterize areas far from the wells location, where the available data is fewer, so one idea still remains: can the seismic data integration within the history matching approach be the solution to this problem?

The integration of seismic data within the history matching helps reducing the spatial uncertainty at locations far from the experimental data (e. g. wells location). However, seismic inversion is an inverse problem with a non-uniqueness solution due to the nonlinear geophysical relation (e. g. the seismic reflection data being an indirect measurement of the subsurface). Another problem concerns the integration of seismic reflection and well-log data in the same support and scale of the reservoir model. Thus, a natural solution is a geostatistical framework which can solve both inverse problems as well as the differences in the scale support. Despite the advantage of dealing with differences in scale support data, within the geostatistical framework it is also possible to assess the uncertainty related to the model parameters and retrieving more reliable reservoir models during this process (Tarantola 2005; Bosch et al. 2010; Caers 2011; Azevedo 2013).

In this work it is presented a new stochastic framework which allows the inference of high resolution reservoir models conditioned simultaneously to: seismic data, well-log data and historical production data without compromising the accuracy of the retrieved subsurface models. An important aspect of the proposed geostatistical history matching is the inclusion of seismic data, i.e. the formulation of a new algorithm that encompasses geostatistical seismic inversion (Soares et al. 2007) within the geostatistical history matching process (Mata-Lima 2008). This is an iterative procedure, where the perturbation is performed recurring to stochastic sequential simulation and co-simulation with joint probability distribution using as patchwork the best matching across multiple stochastic realizations (petro-elastic ensemble simulated at the current iteration). The selection of the petro-elastic models is done based on a multivariate statistical technique, the multidimensional scaling (MDS; Cox and Cox 1994; Scheidt and Caers 2008; Caers 2011; Scheidt 2015), which is able to reveal in few dimensions patterns between a set of multi-dimensional models taking into account the concept of distances by acting as a global optimizer.

1.2. Objectives

This thesis intends to address a relevant problem of the oil and gas industry related with hydrocarbon reservoirs modelling and characterization that is to successfully integrate seismic reflection and production data within the same framework, where the inverted petro-elastic models are able to match simultaneously the observed seismic and the historic production data.

It is proposed a novel approach to history matching techniques with the integration of seismic data. The proposed methodology is applied to synthetic case study, a reservoir with a complex geology (non-stationary geological features - fluvial channels): *Stanford VI* (Castro et al. 2005) since non-stationary sedimentary environment represents a challenging case study for the proposed method. The integration of seismic data into history matching within a geostatistical framework allows to reproduce the key modelling uncertainties captured and quantified in the static modelling, as well as improve the resulting petrophysical models.. Thus, the reservoir models will be able to match the historical production data as well as honour the well-log and seismic data. By honouring all available data, the resulting petro-elastic models have a better chance to correctly predict the reservoir behaviour. The main objectives of this work may be succinctly summarized as following:

- Development and implementation of a new geostatistical history matching methodology with the integration of seismic data into stochastic modelling in an iterative process (both inverse problems within the same framework).
- Apply the initial methodology with different areas of influences around existing wells: (i) same radius size influence for all wells; and (ii) taking into account the deviation of production for each well and the petrophysical parameter of interest from an ensemble of simulations, calculate correlations coefficients (with a integration of a concept of distances).
- Implementation of multidimensional scaling methodology in order to assess the convergence as well as explore the uncertainty space of the stochastic method.
- Obtain more reliable solution for the subsurface Earth model by honouring all data available (well-log data, seismic data and historical production data).

The development and implementation of this novel approach was performed recurring to geostatistical toolboxes from CERENA/CMRP research group and Matlab® (Mathworks). Eclipse® (Schlumberger) was used to set the production strategy for the *Stanford VI* reservoir and for the fluid flow simulations. Petrel ® (Schlumberger) was used to visualize the results.

1.3. Structure of the thesis

This thesis structure comprises six chapters, and it is presented a brief description of each one.

The first and present chapter (Chapter 1) introduces the thesis topic the problem that this thesis tries to solve. It's also discussing the motivation that led to this research and the importance for the industry problems. A brief overview of the implemented methodology and a scope of the work that has already been developed regarding to the thesis topic is presented.

The second chapter (Chapter 2) includes a theoretical overview of the geostatistical topics related with this thesis. It is included a particular attention to the importance of the direct sequential simulation and the direct sequential co-simulation algorithms as part of the inversion procedures within the geostatistical methodologies under the scope of this work.

The third chapter (Chapter 3) presents a detailed description of the developed methodology and the major algorithms that were integrated to accomplish the thesis objectives: the traditional geostatistical history matching and the new algorithm to integrate the seismic data in the geostatistical history matching within the same framework.

The fourth chapter (Chapter 4) is dedicated to the case study description, the results presentation and its discussion.

The fifth chapter (Chapter 5) states the conclusions and summarizes the main findings and contributions of this work.

Finally, the sixth chapter (Chapter 6) refers some suggestions for further research.

Chapter 2. Theoretical Background

2.1. Geostatistical reservoir modelling

Geostatistics can be defined as a tool which aims to study and characterize the spatial or temporal natural phenomena by taking into account the known value of a given property at sparse and discrete locations, as well as quantifying the uncertainty associated to the knowledge of those phenomena (Soares 2006).

Nowadays, the importance of using geostatistical tools as part of reservoir geo-modelling workflow is mainly due to enabling the integration within the same framework of data with different scale support and volume: well-log and seismic reflection data. In early stages of the geostatistical modelling process they are the only available data and while the well-logs are sparsely located along the reservoir and have higher vertical resolution providing trends of the subsurface geological properties by not reproducing the highest and lowest values in areas far away from its locations, the seismic reflection data allows the estimation of the subsurface geological properties in all reservoir extension due to its higher spatial coverage. However, although much more spatial representative, the seismic reflection data only contains indirect measurements of the subsurface geology and its relationship with the subsurface petrophysical properties is non-linear, usually approached as an inverse problem. Therefore, geostatistical tools are the solution in order to obtain resulting models based simultaneously on seismic reflection and well-log allowing more detailed, heterogenic and reliable models (when compared with those models based exclusively from well-log data). Notice that this data have always some noise and measurements errors, so there is an uncertainty associated, which can be taken into account along with the geostatistical process.

There are two main geostatistical techniques used in order to infer the spatial distribution of a given property: deterministic and the stochastic approaches. Deterministic approaches results in a unique solution assuming no uncertainty in the inferred parameter, therefore considering that the inferred model is the true model. These approaches do not address the lack of knowledge regarding the physical system under study and these techniques cannot create the possibility of extreme case scenarios which can have huge impact on forecast the dynamic behavior of the reservoir. On the other hand, stochastic approaches results in an ensemble of equiprobable models based on certain assumptions, such as the prior probability distribution (estimated from the available experimental data) and the spatial continuity model imposed by a variogram or training image allowing simultaneously the assessment of the spatial uncertainty of the inferred property (Soares 2006; Caers 2011).

The next sub-sections explain the geostatistical framework that is the base for the stochastic algorithms used in the new proposed methodology (Chapter 3).

2.1.1. Exploratory data analysis and spatial continuity analysis

Exploratory data analysis is frequently the first step in reservoir modelling and characterization, where each variable is studied recurring to basic statistics such as the analysis of histograms, distribution functions and box-plot. It allows obtaining information regarding central measures: the mean and median; to local measures: the minimum and maximum from quartiles; and measures of spread: variance and interquartile range. Bivariate analysis intends to study the joint behaviour of two variables and for this proposes are usually used *biplots*, bi-histograms and different instruments of regression analysis such as correlation coefficient which measures the linear dependence of two variables.

The second step usually comprises in modelling the spatial continuity pattern that consist on the characterization and quantification of the spatial dispersion of the phenomenon under study from the available experimental data. This step aims is to provide information regarding the spatial dispersion characteristics, such as anisotropy. This is a difficult task when the natural property to be modelled is non-stationary with different trends, because locally the directions of major continuity might change. This study can be performed through mathematical models that assign the properties values to a grid and reflect the conceptualized spatial distribution. A correlogram or variogram represent one possible model of spatial continuity. The variogram (1) and covariance (2) are both measures of the spatial correlation between two data sample dependent on the distance between them, described by $\boldsymbol{h}$, being $\boldsymbol{h} = x_1, x_2 = x_i, x_i + h$. It is possible to measure the geological distances between two points in space, i.e. the similarity among samples for each $\boldsymbol{h}$. Where for a quantitative characteristic $Z(x)$, represented by the pairs of points $Z(x_a)$ and $Z(x_a + h)$ and distanced of h in one direction, all the values measures for each azimuth and lag can be spatially correlated.

$$\gamma(h) = \frac{1}{2N(h)} \sum_{a=1}^{N(h)} [Z(x_a) - Z(x_a + h)]^2 \quad (1)$$

$$C(h) = \frac{1}{N(h)} \sum_{a=1}^{N(h)} [Z(x_a)Z(x_a + h) - m(x_a)m(x_a + h)] \quad (2)$$

Being $Z(x_a)$ the sample value in x_a; $Z(x_a + h)$ the sample value in $x_a + h$; $N(h)$ the number of pairs; and $m = \frac{1}{N}\sum_{i=1}^{N} Z(x_a)$ the arithmetic mean of all realizations composed by N samples, $Z(x_a), a = 1, \dots, N$.

In order to capture the spatial pattern of the unknown reality is necessary to adjust the experimental variogram to a smooth curve, i.e. adjust the experimental variograma to a theoretical model (e.g. spherical, exponential or Gaussian model) able to represent the trend of $\gamma(h)$ related to h as well as being unique and coherent. This adjustment can be done by more than one theoretical model, as such the combination of two theoretical models. Nevertheless, these models have some concepts such as: the range, a, which represents the maximum correlation between the samples and is given by the distance to the sill; the sill, C, that represents the spreading of the variable and by acting as a threshold, from this value the samples are no longer correlated; and the nugget effect representing the small scale variability and turns the variogram different from 0 at $h = 0$. Nevertheless, in order to capture the spatial pattern of the unknown reality it is necessary to adjust the experimental variogram to a smooth curve,

i.e. theoretical model (e.g. spherical, exponential or Gaussian model) able to represent the trend of $\gamma(h)$ related to h as well as being unique and coherent. Furthermore is also possible to adjust more than one theoretical model to the experimental variogram, as such the combination of two theoretical models.

2.1.2. Estimation versus Simulation

The inference of an unknown value,$Z(\boldsymbol{u})^*$ at a certain location $\boldsymbol{u}$ given a set of experimental data can be achieved through two main and different approaches: kriging and sequential stochastic simulation.

Kriging-based techniques estimate the model properties by linear interpolating the values of the experimental data constrained by a spatial continuity model, represented by a variogram in two-point geostatistics. Kriging is able to weight differently isolated samples from clusters samples (declustering). Simple Kriging, Universal Kriging, co-Kriging and Kriging with External Drift are kriging-based interpolators based on the same equation principle (3):

$$Z(\boldsymbol{u})^* - m(\boldsymbol{u}) = \sum_{a=1}^{n(\boldsymbol{u})} \lambda_a(\boldsymbol{u})[Z(\boldsymbol{u}_a) - m(\boldsymbol{u}_a)] \quad (3)$$

Where $\lambda_a(\boldsymbol{u})$ corresponds to the weights given to a specific variable $Z(\boldsymbol{u}_a)$; $m(\boldsymbol{u})$ and $m(\boldsymbol{u}_a)$ are the expected values for $Z(\boldsymbol{u})^*$ and $Z(\boldsymbol{u}_a)$, respectively; $n(\boldsymbol{u})$defines the maximum number of data points that belongs to the set of conditioning data within a neighbourhood around the location $\boldsymbol{u}$. The mathematical details can be found for example in Soares (2006).

The resulting krigged models are smooth representations of the subsurface geology because it tends to reproduce the mean value of the experimental data in areas far away from the location of the experimental data. While the values of the experimental data are honoured, the extreme low and high values of the property of interest are not reproduced far from the location of the experimental data (Deutsch and Journel 1998; Soares 2006).

On the other hand, stochastic sequential simulation algorithms can reproduce all the values retrieved from the experimental data, and so exhibiting small-scale variability, in the models. The joint interpretation from the ensemble of equiprobable models generated within this approach allows the assessment of the spatial uncertainty related with a given property and to analyse the extreme behaviour of this property under some assumptions: the reproduction of the values of the experimental data at its location; the reproduction of the prior probability distribution as estimated from the experimental data; and the reproduction of the spatial continuity pattern imposed by a covariance model (e.g. variogram).

Sequential Gaussian Simulation (SGS; Deutsch and Journel 1998; Goovearts 1997), Sequential Indicator Simulation (SIS; Deutsch and Journel 1998) and Direct Sequential Simulation (DSS; Soares 2001) are stochastic sequential simulation techniques based on the same simulation approach, the Monte Carlo methodology, and the application of the Bayes' rule sequentially. By recurring to Bayes'

theorem it is possible to calculate sequentially the joint probability function (4) from a set of random values $(Z_1, Z_2, \dots, Z_N)$ that corresponds to all the locations available within a reservoir grid.

$$F(Z_1, Z_2, \dots, Z_N) = F(Z_1)F(Z_2|Z_1)F(Z_3|Z_1, Z_2) \dots F(Z_N|Z_1, Z_2, Z_3, \dots, Z_{N-1}) \quad (4)$$

2.1.3. Direct Sequential Simulation (DSS)

The major drawbacks in stochastic sequential simulation algorithms such as SIS and SGS are the requirement of the transformation of the original variables into a set of indicator variables or standard Gaussian variables. As such, among stochastic sequential simulation algorithms the use of the direct sequential simulation algorithm (DSS), as part of the proposed geostatistical framework, overcame that drawback essentially due to its advantage of not requiring any transformation of the original variable (Soares 2001).

Unlike SGS that uses local means and variances by simple kriging estimator to define the local Gaussian conditional distribution function, the DSS uses simple kriging to sample directly from the global conditional distribution function as estimated from the experimental data. In practice, intervals of z are chosen from the cumulative distribution function $F_z(z)$, defining a new $F'_z(z)$ and then simulated values $z^s(x_u)$ are sampled from the chosen distribution $F'_z(z)$, as shown in Figure 1, with intervals centered on the simple kriging estimate $\boldsymbol{z(x_u)^*}$ value with an interval range proportional to the kriging variance, $\boldsymbol{\sigma^2_{sk}}$ (Soares 2001).

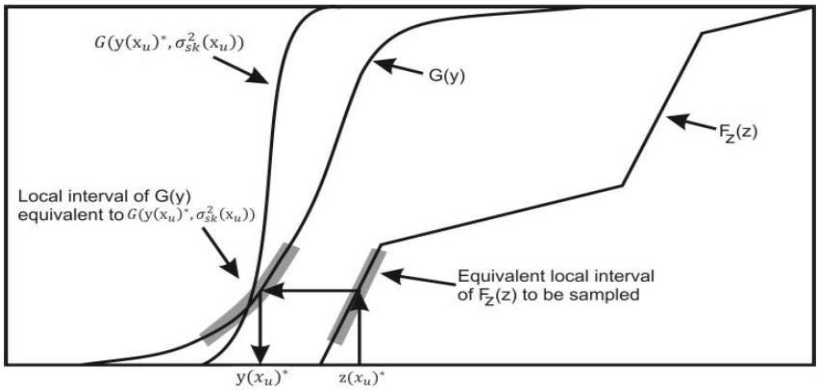

Figure 1 - Sampling of global distribution $\boldsymbol{F_z(z)}$ by intervals defined by the local mean and variance of $\boldsymbol{z(x_u)}$: The value of $\boldsymbol{y(x_u)^*}$ corresponds to the local estimate $\boldsymbol{z(x_u)^*}$. The simulated value $\boldsymbol{z^s(x_u)}$ drawn from the interval of $\boldsymbol{F_z(z)}$ is defined by $\boldsymbol{G(y(x_u)^*, \sigma^2_{sk}(x_u))}$ (adapted from Soares 2001).

The DSS algorithm can be described in the following sequence of steps (Soares 2001):

1. Definition of a random path over the entire simulation grid $x_u, u = 1, \dots, N$, where *N* is the total number of nodes that compose the simulation grid;

2. Estimate the local mean and variance of $\boldsymbol{z(x_u)}$ **-** simple kriging estimate $\boldsymbol{z(x_u)^*}$ and variance $\boldsymbol{\sigma^2_{sk}(x_u)}$ conditioned to the experimental data $\boldsymbol{z(x_i)}$ and previous simulated values $z^s(x_i)$;

3. Definition of the interval of $F_z(z)$ to be sampled, by using the Gaussian distribution law:

$$G(y(x_u)^*; \sigma_{sk}^2(x_u)) \quad \text{with} \quad y(x_u)^* = \varphi(\boldsymbol{z}(x_u)^*) \tag{5}$$

4. Draw a value $z^s(x_u)$ from the cdf $F_z(z)$;
   - Generate a value u from the uniform distribution between [0, 1]
   - Generate a value y^s from $G(y(x_u)^*; \sigma_{sk}^2(x_u))$
   - Return the simulated value $z^s(x_u) = \varphi^{-1}(y^s)$

5. Loop until all N_s nodes have been visited and simulated.

The models resulting from the DSS assumes that the variogram remains stationary across the entire study area. The statistical properties of the conditioning data as inferred from the existing experimental data are also reproduced: local means and variances; the prior probability distribution; and the hard data at its location are respectively honoured.

2.1.4. Direct Sequential co-Simulation (co-DSS)

Direct sequential co-simulation (co-DSS) is an extension of direct sequential simulation that can be applied when two or more variables are spatially depended and (Soares 2001). After obtaining a model of $z_1(x)$ through DSS, the algorithm is applied to $z_2(x)$, assuming the previous simulated model as secondary information with a positive spatial correlation between $z_1(x)$ and $z_2(x)$ characterized by the correlogram $\rho_{1,2}(h)$. The $z_2(x)$ values generated, in any spatial location x_0, from the conditional distribution laws of the previous simulated $z_2(x)$ and $z_1(x)$. Thus, by considering that for the entire space the variables always have the same spatial correlation, i. e. constant value of the correlogram, both variables will reproduce the same spatial statistics patterns, e.g. variogram and global histogram.

The co-DSS algorithm can be described in the following sequence steps:

1) Simulate the secondary variable $z_1(x)$ for the entire simulation grid with DSS;

2) Definition of a random path over the entire simulation grid $x_u, u = 1, \dots, N$, where N is the total number of nodes that compose the simulation grid;

3) Estimate the local mean and variance by using collocated simple co-kriging estimate $([z_2(x_u)^*]_{CSK})$ and the corresponding co-kriging variance $\left(\sigma_{CSK}^2(x_u)\right)$ conditioned to the original experimental data $\left(z_2(x_a)\right)$ the previously simulated values $(z_2(x_a)^*)$ and the value of the secondary variable $(z_1(x_u)^*)$;

4) Definition of the interval $F\left(z_2(x)\right)$ to be sampled, using local mean and variance of the previous point, as shown at figure 1;

5) Draw the value $z_2^1(x_0)$ from the cdf of $F\big(z_2(z)\big)$; (with the same assumptions as previously explained at 5^{th} step of the DSS)

6) Loop until all N_s nodes have been visited and simulated.

2.1.5. Direct Sequential Simulation with Joint Probability Distribution

The limitation of the traditional co-DSS consists in the incapacity of reproducing the same experimental distribution of the original data values in the final bi-distribution of simulated and co-simulated models. In order to solve this problem we may recur to co-DSS with joint probability distributions (Horta and Soares 2010).

The co-DSS with joint probability distributions algorithm ensures the reproduction of the experimental joint probability distribution between the primary and the secondary variables on the simulated models, i.e. the reproduction of the non-linear relationships between properties such as acoustic impedance, porosity and permeability, as well as the reproduction of the experimental bivariate cumulative distribution function between the primary and secondary variables even when the correlation between them is low (Figure 2).

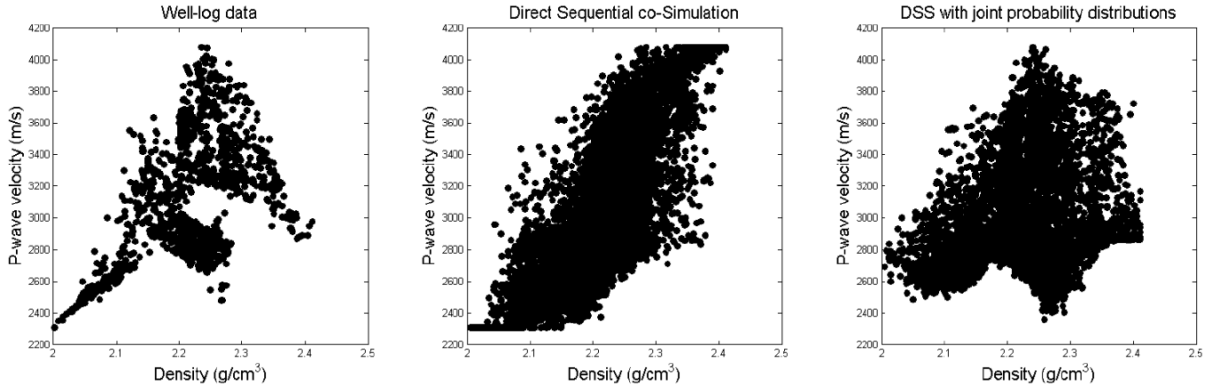

Figure 2 – (from left to right) Joint distributions estimated from well-log data, the resulting bi-distributions between co-simulated models using co-DSS and co-DSS with joint probability distributions, respectively (Azevedo 2013).

The main difference when comparing the traditional co-DSS with co-DSS with joint probability distributions is how the conditional cdf $F\big(z_2(x)|z_1(x)\big)$ is sampled. Horta and Soares (2010) proposed to draw ${z_2}^s(x)$ from the local conditional distribution (6) instead of the global cdf $F\big(z_2(x)|z_1(x)\big)$:

$$F[z_2(u)|z_1(u) = z_1(u)^*] = prob\{z_2(u) < z|z_1(u)^*\}K \quad (6)$$

2.2. Geostatistical Seismic Reflection Data Integration

The characterization of the subsurface geological properties based on well-log data allows the reproduction of highest and lowest values in the wells locations within the geostatistical framework, however it has an incapacity to reproduce them in areas far from those where the uncertainty is higher.

The integration of seismic reflection data in the reservoir modelling process is usually used to estimate the subsurface geological properties allowing reducing the uncertainty in areas far from the wells locations since it gathers large scale information regarding subsurface geology from a much greater reservoir extension when compared with the well-log data, and it is more representative spatially. Its integration within the geo-modelling workflow, usually known as seismic reservoir characterization, can be achieved through the geostatistical framework (previously introduced in Section 2.1). Traditionally, the geo-modelling workflow starts by inferring the subsurface elastic properties (e.g. acoustic and/or elastic properties) as the Figure 3 show.

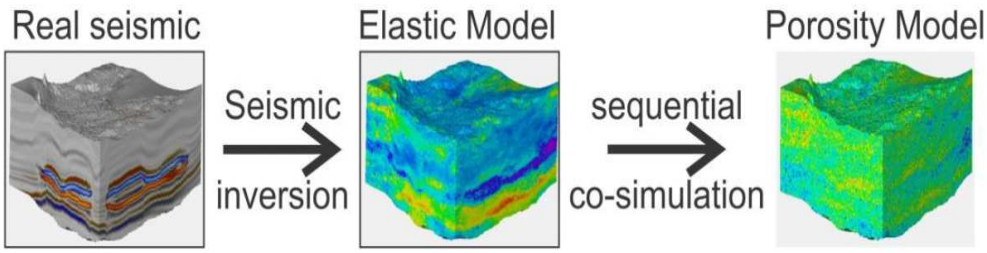

Figure 3 – Schematic representation of the traditional workflow to derive petrophysical models (e.g. porosity) from inverted elastic models (Azevedo 2013).

Transform seismic reflection data into petrophysical properties is an inverse problem, where is only known the response of a particular Earth's system to a limited set of indirect measurements, which tries to infer the parameters of the system in study that give rise to that solution. In practice, seismic inversion problems have some limitations: the limited bandwidth and resolution of the seismic reflection data, noise, measurement errors; physical assumptions and numerical approximations in the forward models; and the uncertainties in estimating a representative wavelet and in the links between reservoir and elastic properties (Tarantola 2005; Bosch et al. 2010).

The indirect geophysical measurements/observations ($\boldsymbol{d_{obs}} \in \boldsymbol{R^s}$) which are normally contaminated by some errors ($\boldsymbol{e}$) originated from different sources and the model parameter space of the subsurface properties of interest ($\boldsymbol{m} \in \boldsymbol{R^n}$) are related by a forward model (F) that may be expressed by (7 (Tarantola 2005):

$$d_{obs} = F(m) + e \tag{7}$$

The forward model, F, can be written in the following form:

$$A = r * w \tag{8}$$

Where A are the recorded seismic amplitudes, r are the subsurface reflections coefficients that are convolved with a wavelet w.

Seismic inversion problems can be divided in two main approaches: deterministic and stochastic methodologies. The seismic inverse problem methodologies review is out of this thesis scope and can be found in Bosch et al (2010). This thesis will only addresses to one specific geostatistical seismic inversion methodology, the global stochastic inversion (Soares et al 2007; Caetano 2009) explained in the next section 2.2.1.

2.2.1. Global Stochastic Inversion (GSI)

The Global Stochastic Inversion (GSI; Soares et al. 2007; Caetano 2009) is an iterative geostatistical methodology based on two main ideas: the used, at the end of each iteration, of a global optimizer based on a genetic algorithm with the cross-over principle; and the perturbation of the inverted models with stochastic sequential simulation (DSS).

The general outline of this iterative geostatistical methodology (Figure 4), GSI, can be described in the following sequence steps (Soares et al. 2007):

1. Generate a set initial 3D images of acoustic impedances by using direct sequential simulation;

2. Create the synthetic seismogram of amplitudes, by convolving the reflectivity coefficients (RC;(9)), derived from acoustic impedances, with a known wavelet;

$$RC = \frac{AI_2 - AI_1}{AI_2 + AI_1} \tag{9}$$

   where the indexes 1 and 2 correspond, respectively, to the mean above and below the interface considered;

3. Evaluate the match of the synthetic seismograms, of the entire 3D image, and the real seismic by computing, for example local correlation coefficients;

4. Ranking the “best” images based on the match (e.g. the average value or a percentile of correlation coefficients for the entire image). From them, one selects the best parts – the columns or the horizons with the best correlation coefficient – of each image. Compose one auxiliary image with the selected “best” parts, for the next simulation step;

5. Generate a new set of images, by direct co-simulation, using the best locals correlation as the local co-regionalization model and return to step 2) starting an iterative process that will end when the match between the synthetic and the real seismic is considered satisfactory or until a given threshold of the objective function is reached.

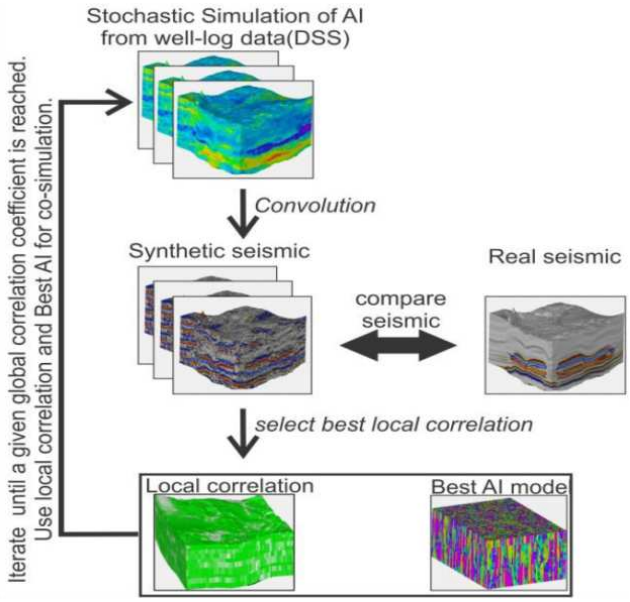

Figure 4 – Schematic representation of the Global Stochastic Inversion methodology (Azevedo 2013).

2.3. History Matching

Reservoir modelling intends to describe the geological and petrophysical description of the hydrocarbon reservoir, i.e. the spatial distribution of its properties such as porosity, permeability and saturations. The static model refers to the reservoir internal properties obtained during its initial characterization generally based on the available information which is mostly discrete, sparse and with different support volume and resolution (well-log and seismic reflection data), and it is usually integrated through geostatistical tools such as stochastic sequential simulation (DSS and co-DSS). However, the hydrocarbon reservoir is not static but dynamic since it contains fluids, i.e. after the initial petrophysical characterization (e.g. porosity and permeability) the resulting petrophysical models are used as input for the process of reservoir fluid flow simulation where its dynamic response to the reservoir internal properties are assessed. This dynamic response refers to temporal data resultant from the fluid flow behavior to the reservoir's internal properties, usually known as dynamic modelling (Section 2.3.1). The dynamic data can be inferred from the static model or known from the wells (rates, pressure, etc.). The integration of dynamic data into petrophysical models of petroleum reservoirs is usually conducted by history matching techniques (section 2.3.2) which allows the calibration of the static model to the known dynamic data.

The history matching is an inverse problem which aims to obtain the internal petrophysical reservoir properties model able to reproduce the well-log data and seismic surveys (static model) as well the fluid behaviour that takes into account the known dynamic data, i.e. historical production data, by tuning the reservoir models to match the historic production data (Mata-Lima 2008). The difficulty within the history matching process resides on the highly non-linear relationship between the model response and the parameters. More troubling, however, is the consistency between the static input data and the resulting reservoir model that is often lost in a traditional history matching phase, especially if it is treated as a curve fitting exercise. Therefore, in order to obtain more consistent reservoir models, the match towards

the integration of all prior knowledge (e.g. well-log, seismic data, etc.) in the static modelling stage is very important as well as its dynamic response within the reservoir simulation stage, that is submitted to evaluation throughout an objective function (Section 2.3.3) by taking into account the history production data. The perturbation of the model parameter space in order to match the available production data only stops until a minimum value for a given objective function is achieved, i.e. until the simulator is able to reproduce the known reality, such as pressure, production level and water-cut.

2.3.1. Dynamic modelling

The fluid flow simulation is run on the resulting petrophysical models, i.e. on the static model, and its response can be translated in terms of rates and pressures. Dynamic modelling is based on the relationship of balance between what enters less what exists in a defined volume and what is produced and accumulated from the same volume. Thus, by relating the production rates with the rock and fluid properties such as porosity and permeability, it is possible to predict the reservoir behaviour, which is the main objective of dynamic modelling.

The reservoir simulator creates mathematical models of the physical reality of the reservoir and the dynamic processes that are the base for the production where the fluid flow simulation is performed using large finite difference simulators in order to solve conservation equations that describe the multi-phase flow through the porous reservoir rocks (Figure 5). The Darcy's equation (10) is the basic equation of the system of equation of finite differences which is solved during the increment of the time:

$$Q = \frac{k \times A \times \Delta p}{\mu \times L} \tag{10}$$

Where Q is the flux caudal of a fluid, k is the permeability of the porous environment, A is the available section for the fluid flux, Δp pressure difference between blocks, μ is the viscosity and L the distance between the centre of the blocks.

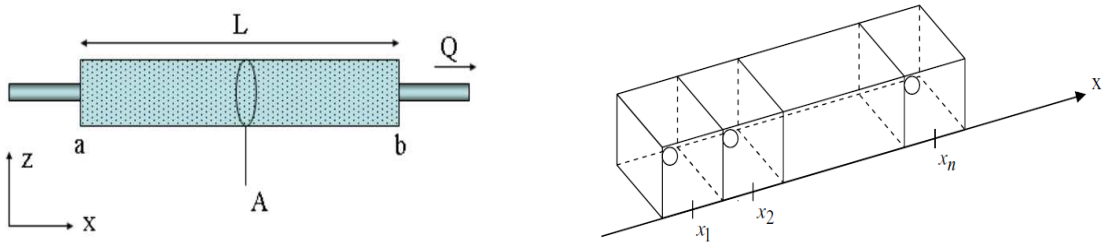

Figure 5 –Constrained fluid within a porous environment with higher pressure in **a** than in **b**, so the fluid flows through **b** direction; Block center in a unidimensional grid (Adapted from Carneiro, J. 2010)

The reservoir simulation is a valuable tool to evaluate and validate the models generated during the static modelling stage. Under the scope of this thesis, Eclipse 100 Black Oil Simulator® (Schlumberger) was used as the fluid flow simulation.

2.3.2. Classical approach to History Matching

History matching can be defined as the exercise of adjusting the model properties to the production historical data, where the result is known but the conditions that originate such result are unknown. History matching is also known as a process to calibrate the initial reservoir model to the historical production data. The dynamic response of the resulting petrophysical models simulated is evaluated when compared with the real historical production data by taking account dynamic parameters such as pressure, production level and water-cut. Therefore, in order to adjust the model properties to the historical production data the model parameter space is perturbed by recurring to an objective function which represents the discrepancy between the observed and the simulated data, until a minimum value for a given objective function is achieved (Gomes and Alves 2013; Caeiro 2014).

Traditionally, history matching was performed to one single deterministic model where the spatial uncertainty of the modelled properties was not considered. As consequence, key modelling uncertainties captured and quantified in the static data conditioning using geostatistical tools have been often lost in the history matching phase. Thus, to reflect the uncertainty of the model within the history matching procedure, new techniques started to be developed aiming the generation of multiple history matching models (Hoffman 2005). Since the 90's with the recognition of the importance to assess the uncertainty by examining multiple models (Tyler, 1993), different authors tried to solve this problem by recurring to stochastic sequential simulation algorithms in order to perturb the parameter space model due to its simplicity of implementation, such as Gradual deformation (Roggero and Hu 1998; Hu et al. 2001), Probability perturbation (Caers and Hoffman 2006) and Co-simulation (Mata-Lima 2008; Le Ravalec-Dupin 2011). The main idea behind most history matching procedures is to perturb the model parameter space following the next sequence of steps (Figure 6):

1. Reservoir models are created by taking into account the prior knowledge and observations from the wells (e.g. porosity and permeability) which try to describe the spatial distribution of the subsurface properties of interest;

2. Dynamic simulation is run on the previous models to obtain the simulated production history per well;

3. Comparison between the simulated historical production data from each model and the real historical production data through an objective function. The simulated model that minimizes this objective function within an acceptable interval is accepted;

4. Create a perturbation in the initial model with the information obtained from the objective function and repeats all the previous steps until a minimum value of the objective function is achieved.

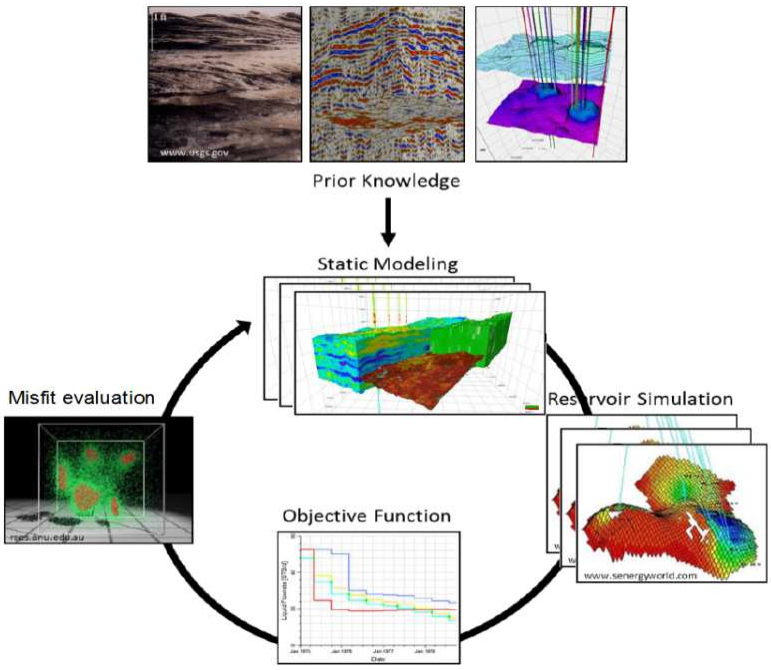

Figure 6 – General framework of history matching (Adapted from Caeiro, 2014)

Within this thesis novel approach to history matching problems tries to match simultaneously the observed seismic reflection and historical production data where the areas of influence of each well are constrained differently and generates different outcomes. The perturbation of the models parameters space will be performed recurring to stochastic sequential simulation and co-simulation: direct sequential simulation and direct sequential co-simulation with joint probability distributions; after being evaluated through the multidimensional scaling. This thesis implementation is explained in detail in Chapter 3.

2.3.3. Objective function and misfit value

An objective function is a mathematical expression which measures the match between the true observed production time and the production retrieved by the fluid flow simulation. Usually, this value is minimized by the algorithm which founds a model that better fits the observed data. The comparison of simulated and observed data can also be expressed as a misfit function in case of assisted history matching procedure, which is in fact, if translated into an optimization problem, an objective function (Christie et al. 2013; Caeiro 2014) .

Commonly, the most applied objective function in history matching methods basis on a single number, the misfit or match quality (Mf), which is obtained by summing the least square misfits for all the quantities of interest in a history match (11).

$$Mf = \frac{1}{2}\sum_{i=0}^{N}\frac{(obs_i - sim_i)^2}{\sigma_i^2} \tag{11}$$

Where, at time=i, obs_i is the observed or historical data (e.g. rate or pressure) and sim_i is the simulated results. *N* refers to the number of measurements (the amount of time steps where the measurement was made) and σ_i the measurement error in the observed data (goodness function).

Within an optimised history matching procedure the use of the objective function can be expressed as a multi-objective function, where different parameters are taken into account and when summed together performed as a global objective function. This global objective function is able to comprise targets with different scales by combining all the evaluated parameters and thereby obtaining an optimization problem which in practice is reduced to one variable. The main drawback within this approach concerns to the possible conflict between optimization variables, i.e. the better adjustment in one cannot necessarily be a good adjustment on another variable (Carneiro 2010).

Chapter 3. Geostatistical history matching integrating seismic reflection data

Generating Earth models able to fit both recorded seismic reflection and historic production data is an essential step for more reliable hydrocarbon reservoir characterization and reservoir's forecast. Commonly, both processes are approached in separate workflows where each type of data is matched individually (Azevedo 2013). The petro-elastic models obtained from geostatistical seismic inversion algorithms (e.g. GSI; Section 2.2) are able to match the observed seismic reflection data, however in mature fields they may start to show some incapacity within the history matching process (Section 2.3). Therefore while tuning the reservoir models to match the observed production data, the resulting petro-elastic models may start to diverge from the observed seismic reflection data. This is more evident at locations far from the wells, where the constraining data is fewer. Therefore in order to build reliable reservoir petrophysical models it imply the integration of seismic reflection data during history matching since it allows the coverage of the entire reservoir extent and provides a better geological consistency along with the well-log data. This thesis proposes a geostatistical history matching methodology where the seismic data is integrated as part of the history matching procedure.

The methodology presented herein can be divided in two approaches: the geostatistical history matching (Section 3.1) and the geostatistical history matching with seismic data integration (Section 3.2). The general framework of the proposed methodology is depicted in Figure 7 and both procedures are outlined in the following sections. This integrated methodology is based on a genetic algorithm, acting as a global optimizer, where the selection of the conditioning data for the next iterations is based on the petro-elastic ensemble simulated at the current iteration with better response in the MDS and the perturbation of the models parameters is performed recurring to stochastic sequential simulation and co-simulation.

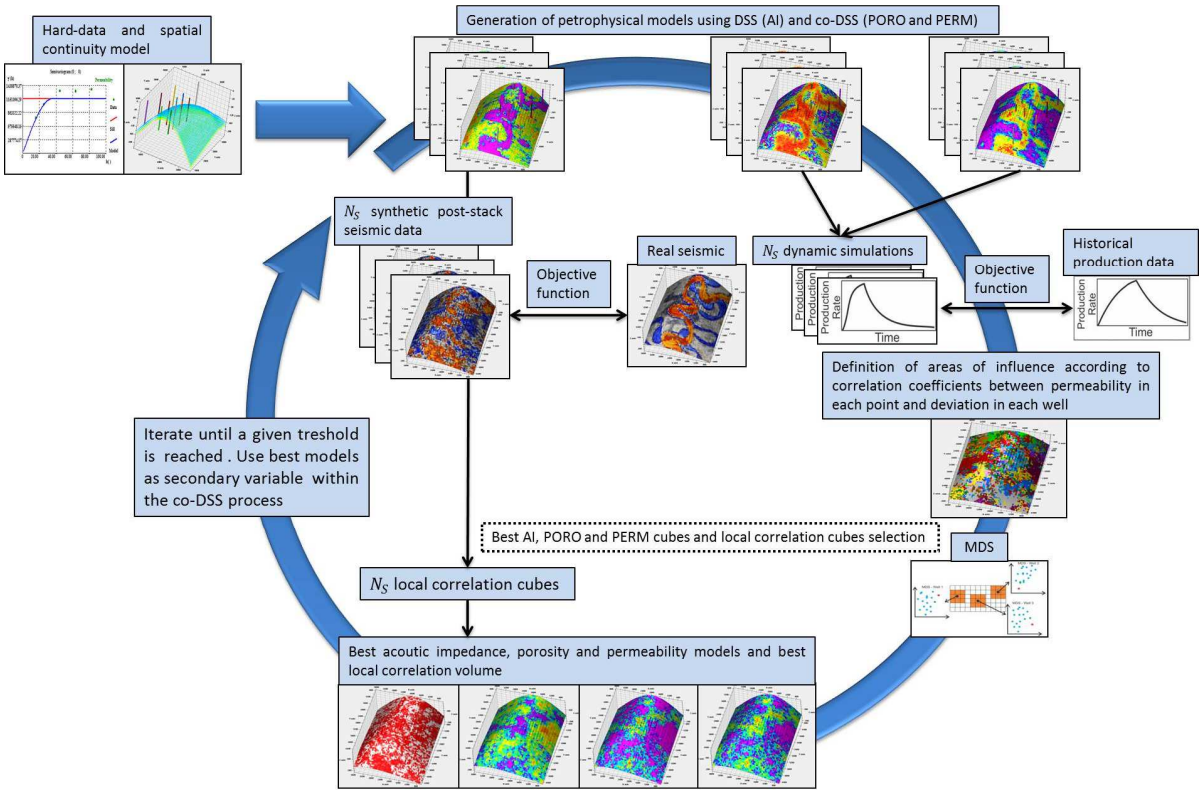

Figure 7 – General framework of the proposed methodology with the integration of seismic data.

3.1. Geostatistical History Matching

Historical production data is usually integrated by inverse methods which involves the perturbation of the model parameter space until the match of the simulated production response towards the historical production data is reached. The discrepancy between simulated and historical production data is evaluated recurring to an objective function and is minimized during the optimization process. The perturbation approach within the geostatistical history matching is performed in the reservoir properties so the complex processes of the fluid flow simulation may be reproduced.

The stochastic modelling is applied using DSS (Section 2.1.3) and co-DSS (Section 2.1.4) algorithms to model the internal petrophysical properties of the reservoir (porosity and permeability). The deterministic dynamic modelling was implemented resorting to Eclipse® 100 Black Oil (Schlumberger) software. The dynamic simulation allow to know the information about the direct response of the fluid flow in the reservoir for the input data considered, as well as to know more about the petrophysical properties not sampled in the reservoir, by relating the production rates with the rock and fluid properties: porosity and permeability with oil and water.

Mata-Lima et al. (2007) developed one way to integrate dynamic data into the reservoir modelling process within a geostatistical framework. This methodology guarantees the preservation of the imposed spatial pattern as inferred by a variogram model. This approach may be summarized by the following sequence of steps (Figure 8):

1) Generation of a set of models for reservoir petrophysical property using DSS;

2) For each generated model perform the dynamic simulation in order to obtain a simulated historical production data - Eclipse® 100 Black Oil (Schlumberger);

3) Comparison between the simulated historical production data from each realization and the real historical production data, where the discrepancy between them is evaluated through an objective function at each different time (*timestep*). The simulation that minimizes this objective function is accepted.

4) Create a perturbation, by co-DSS, in the initial model with the information obtained from the objective function and repeats all the previous steps until a minimum value of the objective function is achieved.

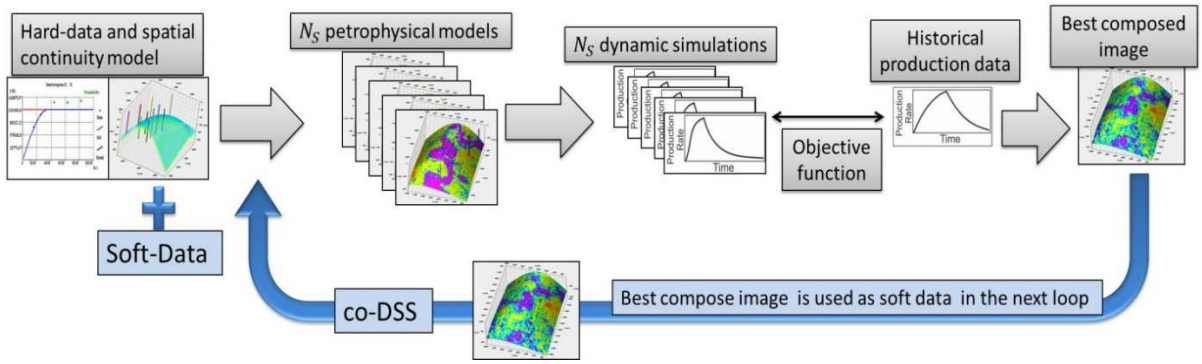

Figure 8 –Geostatistical history matching workflow.

This methodology allows the generation of multiple petrophysical models that honours the information from the wells (static data from well-logs) as well as the generation of a set of models which are able to reproduce the real historical production data from the production wells. As the iterative process evolves the difference between simulated and observed production data will decrease and preserving the imposed pattern of spatial continuity from the variogram model in the resulting simulated models.

The implementation of this methodology is firstly based on the prior information obtained essentially from well-log data. The study of well-log data values and spatial continuity allows to assume the properties distribution and the spatial continuity pattern (imposed by the variogram model) of the reservoir at the same time. By taking into account the initial study regarding the prior information it is performed the stochastic sequential simulation algorithm, DSS, by generating N_s equiprobable petrophysical models. Then, through the dynamic response obtained from the dynamic fluid flow simulation of each simulated model is possible to evaluate how well the model can reproduce the real historic production data by recurring to an objective function. The simulated model with lowest misfit will be used as secondary variable for the co-simulation for the next iteration. While perturbing the model parameter space with the generation of new reservoir models using the previous simulation model as soft data, this iterative process aims to achieve a faster convergence of the resulting models by decreasing the difference between simulated and observed historical production data.

In order to improve the efficiency of this methodology, allowing a faster convergence, two alternative methods were implemented when compared against the conventional approach (Mata-Lima 2008): (i) the multi-criteria objective function and (ii) the local perturbation. By taking into account the values of pressure and water production from each well for each time, the multi-criteria objective function (12) comprise the information regarding each production well and tries to match the response of the entire set. The misfit depends on the variable of interest from the production wells: well bottom hole pressure, WBHP; the well water production rate, WWPR; and on the time steps (Figure 9). The multi-criteria objective function, M, applied in this geostatistical history matching methodology consist the minimization of the function:

$$M = \sum wells \sum WBHP, WWPR \sum time \frac{\left(q_{ijk}^{obs} - q_{ijk}^{sim}\right)^2}{2\sigma_{ij}^2} \quad (12)$$

where q_{ijk}^{obs} are the observed values, q_{ijk}^{sim} are the simulated values, σ_{ij}^2 the data variance, WBHP the well bottom hole pressure, and WWPR the well water production rate.

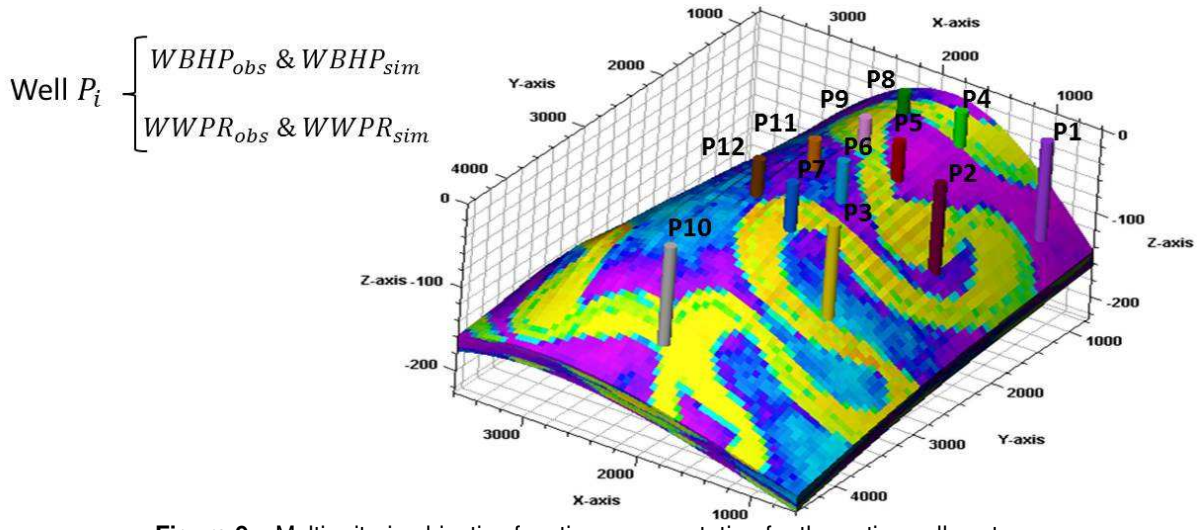

Figure 9 – Multi-criteria objective function representation for the entire wells set.

The local perturbation consists on a regional perturbation achieved locally by defining influence zones around each well (Figure 10). This methodology can be applied when the available dynamic data refers to more than one producer well. While performing the regional perturbation, a best compose image is reached. The objective of using this best composed image is to define patches around each well and the realizations with lower misfit from each patch are merged together. The images with the closest dynamic response are calculated by the previous objective function by taking into account the dynamic data per well.

The definition of the areas of influence from each well can be critical since it may allow the selection of the reservoir grid cells that should be perturbed in order to match the observed production data, leading to faster convergence and reduced computationally costs of the fluid flow simulation. Furthermore, this methodology is very simple to implement since with these changes it is also achieved a faster convergence of the objective function, allowing to obtain better results and more reliable models with higher consistency, by honoring the initial data and keeping the same spatial pattern as revealed by a

variogram model. The patchwork model is only used as secondary information, i.e. soft data in the next iterative process, and do not guarantee the spatial continuity and the connectivity of the channels such as the original images.

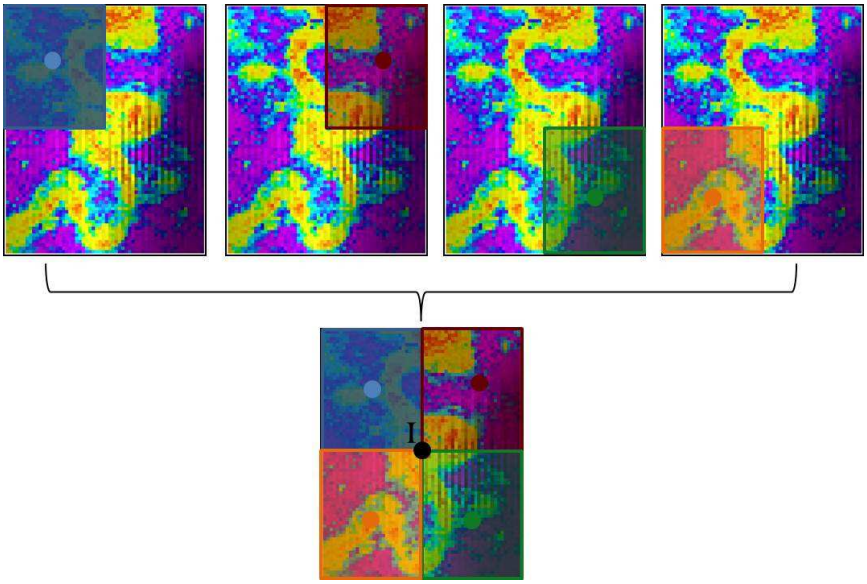

Figure 10 – Best composed image representation applied to a reservoir were the wells distribution comprises a five spot strategy (4 producer wells and 1 injector well).

The criteria proposed in Mata-Lima (2008) consists into a symmetric division of the reservoir space for each well constraining all the reservoir to match towards the historical production data. One of the problems related history matching is the loss of prior information by tuning the reservoir petrophysical properties, i.e. the loss of the properties spatial continuity pattern. As a consequence, the consistency between the static data and the resulting simulated models may not be reproduced. Therefore, in order to tackle this problem, it is proposed a new way to define the areas of influence, according to: (i) geometric criteria and (ii) correlation coefficients between the ensemble of the petrophysical properties and the deviations between real and simulated production responses. Thus, by considering different definitions of areas of influence and with the seismic data integration (Section 3.2) is possible to guarantee a better reproduction of the reservoir properties by matching not only the historic production data but also the observed seismic reflection data.

3.2. Geostatistical History Matching with Seismic data integration

Geostatistical approaches for integrating production into reservoir modelling and characterization try to incorporate the prior geological knowledge about the spatial distribution of the reservoir's petrophysical internal properties, as well as the reservoir's engineering parameters (e.g. SCAL and PVT conditions). Mata-Lima (2008) proposed a geostatistical history matching methodology (Section 3.1) where the reservoir model is regionalized in areas of influence taking into account the location of the available wells by a geometric criteria. However, besides its simplicity of implementation and faster convergence

while the model parameter space is tuned to match the observed production data, the resulting petro-elastic models may start to diverge from the observed seismic data. This is more evident at locations far from the wells, where the constraining data is fewer, making this models less suitable to predict the reservoir behaviour since the misfit between observed and simulated production data are only known at sparse locations (well locations). Thus, in order to obtain reservoir models able to reproduce with lower uncertainty and hopefully more reliable, it is proposed within this thesis a novel geostatistical history matching methodology where the seismic reflection data is integrated as part of the history matching procedure.

The geostatistical history matching with seismic data integration is an iterative procedure based on a genetic algorithm, acting as a global optimizer, where the perturbation of the models parameters is performed recurring to stochastic sequential simulation and co-simulation. The proposed workflow may be divided in three different stages: (i) the stochastic simulation of petro-elastic models, forward modelling and the comparison against the observed seismic reflection and production data (Figure 11); (ii) the definition of areas of influence according to geometric criteria, the definition of influence areas according to correlation coefficients between the ensemble of the petrophysical properties and the deviations between real and simulated production responses; and (iii) the selection of the conditioning data for the next iterations based on the petro-elastic ensemble simulated at the current iteration.

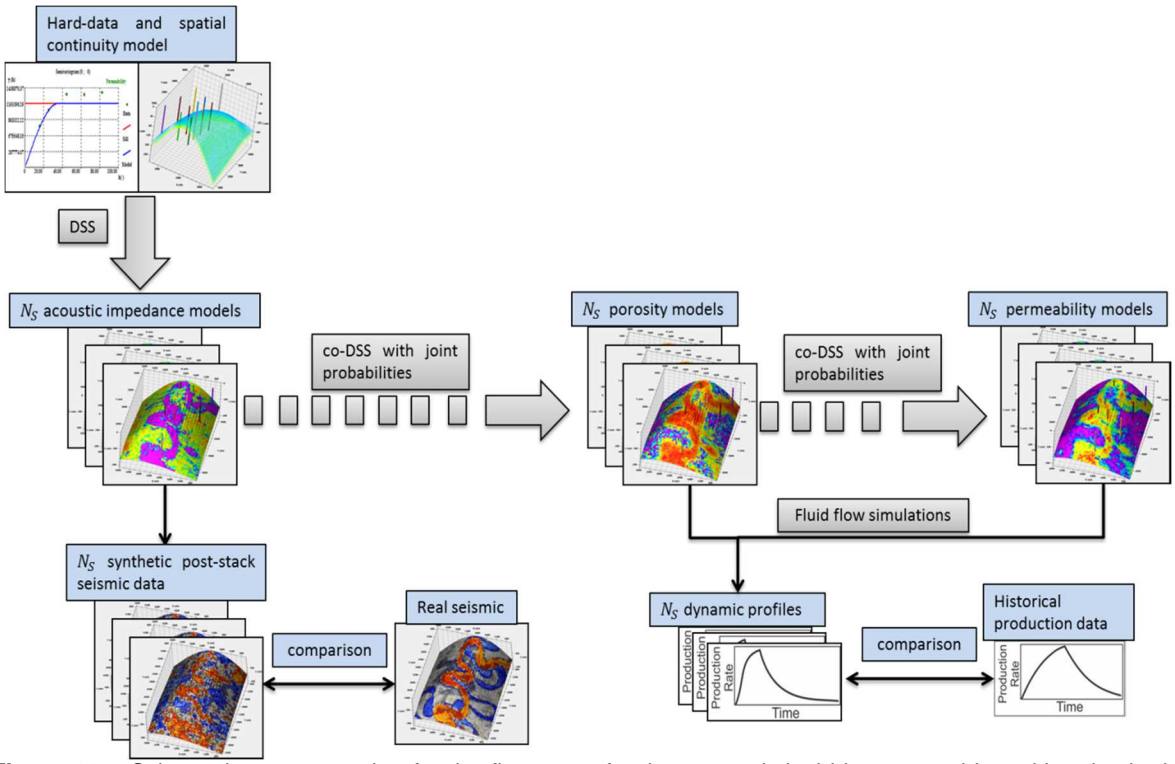

Figure 11 – Schematic representation for the first stage for the geostatistical history matching with seismic data integration.

First, an ensemble of N_s acoustic impedance models is simulated with DSS (Soares 2001) by taking into account the hard-data and a spatial continuity model as expressed by a variogram model. Each impedance model is used as secondary variable for the co-simulation of N_s porosity models, through

the co-DSS with joint probability distributions (Horta et al. 2010). The simulation sequence finishes with the co-simulation of N_s permeability models using the previously simulated N_s porosity models as secondary variables, with co-DSS with joint probability distributions (Horta et al. 2010).

The seismic forward modelling stage comprises the following steps: the N_s post-stack synthetic seismic volumes are computed based on the ensemble of N_s acoustic impedance models; and the calculated reflection coefficients assuming normal incidence are then convolved by an estimated wavelet for the reservoir area.

The comparison between each synthetic volume and the real seismic reflection data is obtained in terms of correlation coefficient, in a trace-by-trace basis, and the resulting local correlation coefficients are then stored in N_s local correlation cubes. The local correlation coefficients may be translated as seismic deviations from the recorded seismic data:

$$e_s^l = (A^l - A_r), l = 1, \dots, N_s \quad (13)$$

where A^l is the synthetic seismic data and A_r is the real seismic reflection data.

The resulting N_s duplets of porosity and permeability from co-simulation are used as input for a fluid flow simulator, Eclipse® 100 Black Oil (Schlumberger), while the seismic forward modelling is being performed. From the fluid flow simulation results N_s production profiles for the variables of interest (e.g. oil and water production) and depending on the target of the history matching (e.g. well pressure and production rates) the simulated responses are compared towards the observed historical production data. From each simulated production profile N_s deviations from the observed historical production data may be computed as follow:

$$e_d^l = (d^l - d_r), l = 1, \dots, N_s \quad (14)$$

where d^l is the synthetic production profile and d_r is the observed historical production data.

During this first stage is possible to assess the mismatch between synthetic and real seismic reflection data as well as the deviations between simulated and observed historical production data.

The second stage concerns the definition of areas of influence for each well, which is not simple and may be defined recurring to different methodologies. The simplest one is the definition according to geometric criteria such as a circular area with a fixed radius around each well location. This radius can be set equally for all the available wells or with different dimensions, since wells located in clusters will probably reflect smaller individual areas of influence while isolated wells may reflect higher areas of influence.

Another approach to define the areas of influence for each well, proposed under the scope of this thesis, is based according to the correlation coefficients between the petrophysical properties of interest (e.g. permeability and porosity) in a given point within the reservoir grid and the production deviation in a well.

By assuming $Z = Z(x)$ to be a petrophysical parameter of interest such as permeability or porosity, known at N_W sparse spatial locations x; and considering as state variables the normalized absolute

mean deviation between the N_s dynamic responses and the observed dynamic response at each well, averaged through all the time steps (15), $Y(x_\alpha), x_a = 1, \dots, N_W$, it is possible to calculate the correlation coefficients (16), $C\big(Z(x), Y(x_\alpha)\big)$, through the ensemble of simulation:

$$Y_\alpha = \frac{1}{median(real\ production)} \times \frac{1}{N_T} \sum_{T}^{N_T} |simulate\ production - real\ production| \tag{15}$$

$$\rho_{Z,Y} = \frac{cov(Z,Y)}{\sigma_Z \sigma_Y} \tag{16}$$

The resulting correlation coefficients can be though as indicators of the relationship between the petrophysical parameter Z in each point x of the grid and the dynamic deviations in each one of the wells. Thus, areas highly correlated with a given well are more likely to be related with the historical production data of that well, i.e. areas with high correlation coefficient are those where the permeability play a key role for the production of that well and by this way dividing the grid into regions. The use of these correlation coefficients can be used as a spatial indicator of the relation between the dynamic responses and the petrophysical parameters since the absolute highest values are mainly located in the neighbourhood of the wells, therefore defining the areas of influence of each well. This areas of influence are calculated as a simple kriging process (17) at the end of each iteration since the correlation coefficients are different at each iteration and consequently the calculated areas of influence of each well.

$$Z(x)^* - m(x) = \sum_{\alpha=1}^{n(x)} \lambda_\alpha(x)[Z(x_\alpha) - m(x_\alpha)] \tag{17}$$

Where λ is the kriging weight and $Z = Z(x)$ is the petrophysical parameter of interest such as permeability, known at sparse spatial locations x; and m the normalized absolute mean deviation between the N_s dynamic responses and the observed dynamic response at each well, averaged through all the time steps, $x_a = 1, \dots, n(x)$.

However, since the correlation coefficients may be high in areas with low feasibility of being influenced by a given well, i.e. areas far from the wells locations are constrained in terms of proximity. The correlation coefficients from each well are related based on a concept of distances, where the ones far from the wells locations have less weight and the near ones higher weight in order to achieve convergence for each one of the wells.

The third stage consists on the selection of the best models of acoustic impedance, porosity, permeability and the best local correlation coefficients at the end of a given iteration. These models are going to be used as seed, soft data, for the generation of a new set of models during the next iteration. These models are patchwork models created through the selection of best-fit regions from the set of simulated models which ensure the lowest misfit between observed and synthetic data for both, recorded seismic reflection and observed historical production data.

Since the seismic reflection data covers a great spatial extent of the reservoir grid and the production responses at wells location are highly dependent of the model parameters, the selection of the petro-elastic models that are going to fill the areas of influence of each well is done by plotting the synthetic seismic reflection data and the simulated production responses with real one in a multidimensional scaling referential.

Multidimensional scaling is a multivariate statistical technique able to reveal in few dimensions patterns between a set of multi-dimensional models based on the concept of distances (Caers 2011). The MDS consists on the conversion of the dissimilarity matrix (D) into points which are then plotted in a Cartesian space, where the matrix D is first converted into a matrix A by a scalar product. After, A is decomposed by eigenvector decomposition where only the first d principal components (eigenvectors) are retained (Cox and Cox 1994; Borg et al. 1997; Caers 2011).

Within the MDS procedure it is essential to define the distance used in order to construct the dissimilarity matrix (D), i.e. the relative position between simulated models and the real one in the metric space, therefore reflecting the similitude between all models. Thus, depending on the type of data the distances may vary: the Hausdorff distance may be suitable in case of bodies with different shapes, and in case of different temporal signals such as seismic reflection data, correlation-based distances may be more suitable (Scheidt and Caers 2008; Azevedo 2013). For the geostatistical history matching with seismic data integration, the proposed distance is based on a multi-criteria objective function (Mf; (**18**), which reflects the match between the observed and synthetic data for both, recorded seismic reflection and observed historical production data:

$$Mf = W_{sy} \times \sqrt{\sum_{i,j=1}^{N_s} \frac{1-\left(\rho_{ir}+\rho_{jr}\right)}{2}} + W_{dy} \times \sum_{i,j=1}^{N_s} \frac{\left(x_{ir}-x_{jr}\right)^2}{2\sigma_i^2}, r = 1, \dots, R \quad (18)$$

Where R is the total number of wells, the ρ_{ir} and ρ_{jr}, and the x_{ir} and x_{jr} are both responses of the ensemble of models comprising the N_s simulated seismic and production models with the real seismic reflection data and the historical production data respectively for a given well (r); σ_i is the deviation assumed for the historical production data; W_{sy} and W_{dy} are user-defined weights defined for seismic and dynamic data respectively.

Note that within this space, the MDS space, similar models will be plotted in a cluster while distinct models will be plotted with greater distances among themselves. The distance matrix (D) is calculated taking into account the distance between simulated petro-elastic models and the real model, considering the simulated and observed seismic reflection and historic production data. The petro-elastic models with shorter distance relative to simultaneously the observed seismic reflection and historic production data will be stored to build the best acoustic impedance, porosity and permeability within the respective area of influence of each well, while the associated local correlation coefficients computed between synthetic and real seismic will be stored in a local correlation cube.

The portions of elastic models, from the N_s models simulated at the current iteration, which produce synthetic seismic with the highest correlation coefficients when compared with the real seismic data are stored in the best acoustic impedance, while the best porosity and permeability models are constructed with the corresponding patches as selected for the best acoustic impedance.

The geostatistical iterative procedure continues with the generations of a new set of petro-elastic models recurring to co-simulation and using the best acoustic impedance, porosity and permeability as secondary variables along with the best local correlation volume. This procedure is considered finished when it is achieved a certain threshold regarding the global correlation coefficient between synthetic and observed seismic data.

The geostatistical history matching with seismic data integration can be summarized by the following sequence of steps (Figure 12):

1) Stochastic simulation of N_s acoustic impedance models using DSS;

2) Co-simulation of N_s porosity models with co-DSS with joint probability distributions using the previously models simulated 1) as secondary variable;

3) Co-simulation of N_s permeability models with co-DSS with joint probability distributions using the previously models simulated 2) as secondary variable;

4) For each model simulated in the first step 1) compute N_s synthetic seismic volumes and compare each one with the real seismic in a trace-by-trace basis;

5) For each duplet of porosity and permeability 2) and 3) run the respective fluid flow simulations using Eclipse® 100 Black Oil (Schlumberger), and compare the simulated responses towards the observed historical production data;

6) Definition of areas of influence according to correlation coefficients between permeability in each point and deviation in each well;

7) Plot the correlation coefficients between the real and simulated seismic reflection, as well as the plot of the real historic production data and the simulated historical production data.

8) Plot the observed and simulated data for both, recorded seismic reflection and observed historical production data, in the MDS space for each well individually;

9) The inverted petro-elastic models with shorter distance relative to simultaneously the observed seismic reflection and historic production data will be stored to build the best acoustic impedance, porosity and permeability within the respective area of influence of each well, while

the associated local correlation coefficients computed between synthetic and real seismic will be stored in a local correlation cube.

10) The portions of elastic models, from the N_s models simulated at the current iteration, which produce synthetic seismic with the highest correlation coefficients when compared with the real seismic data are stored in the best acoustic impedance, while the best porosity and permeability models are constructed with the corresponding patches as selected for the best acoustic impedance.

11) Based on a global genetic algorithm, the "best" models created in the previous step 7) are used as secondary variable in the perturbation of the model parameters recurring to co-DSS. Return to the first step 1) and iterate until a certain threshold regarding the global correlation between synthetic and observed seismic data is reached.

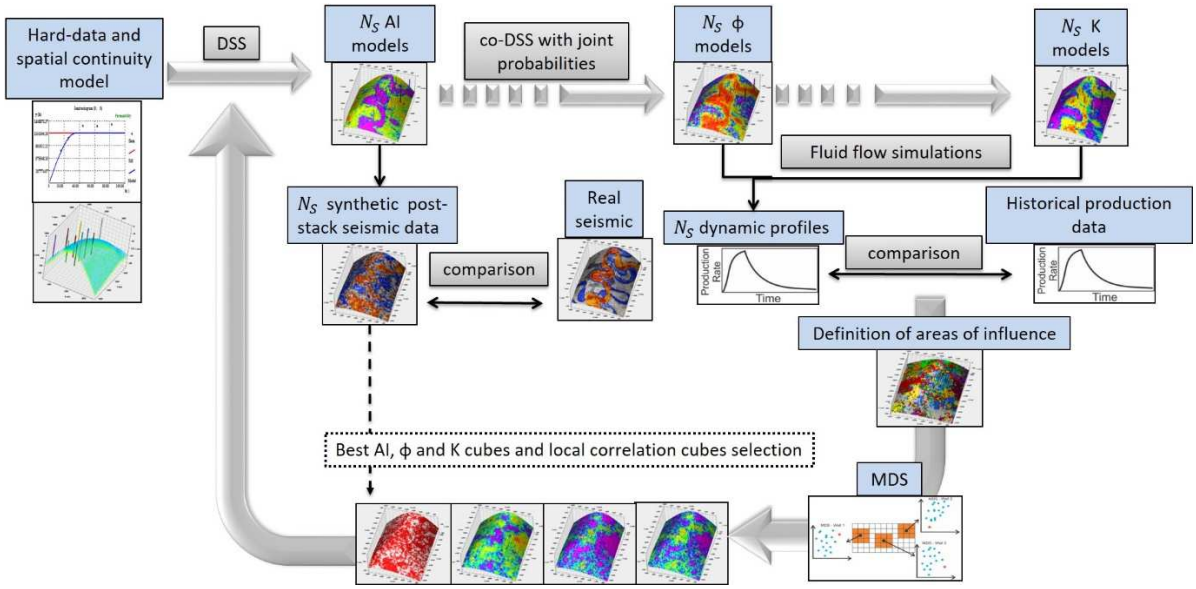

Figure 12 - Schematic representation of the geostatistical history matching with seismic data integration.

Chapter 4. Case study

The proposed methodology was tested and implemented in a synthetic case study. The results are is presented in this section to illustrate the applicability of the methodology previously introduced in Chapter 3. This synthetic reservoir exhibits a realistic exhaustive sampling of petrophysical properties and a realistic fluid flow simulation and has been widely used to test history matching procedures.

4.1. Reservoir Description

The 3D synthetic reservoir, the Stanford VI reservoir (SVI; Castro et al. 2005), and the stratigraphic model corresponds to a fluvial channel system, divided into three layers: Layer 1, sinuous channels with 80 meters thick; Layer 2, meandering channels with 40 meters thick; and Layer 3, delta front with 80 meters thick.

For this specific study only Layer 2 of the SVI was considered. The reservoir is an asymmetric anticline with axis N15Eº comprising meandering channels of variable sizes with four facies types: floodplain, point bar, channel and boundaries; and no faulting, composed by 6million cells $(150 \times 200 \times 200)$ where each cell as the dimension of $25 \times 25 \times 1$ meters in the *i, j, k* directions, respectively, which mean that the reservoir is 3.75 Km wide (East-West) and 5.0 Km long (North-South). However, in order to speed-up the fluid flow simulator, one of challenges of the proposed iterative methodology, the original reservoir was upscale into a new grid composed by 90 thousand cells $(60 \times 75 \times 20)$ where each cell as the dimension of $50 \times 50 \times 2$ meters in the *i, j, k* directions, respectively (Castro et al. 2005).

The original synthetic dataset, assumed as real data within this thesis, is composed by a set of 23 wells from where only 12 were used to constraint the geological history matching with seismic data integration, while the rest of the wells were not used in any part of the procedure (Figure 13). The dataset comprises, along with the well set, the true three-dimensional models of acoustic impedance, porosity and permeability as well as a noise-free full-stack seismic volume (Figure 14).

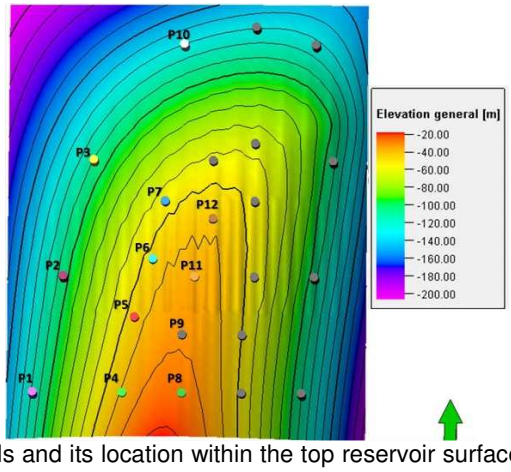

Figure 13 – Available set of wells and its location within the top reservoir surface study area (SVI). Colored wells are the ones used to constraint the geostatistical history matching with seismic data integration, while the black filled wells were not used.

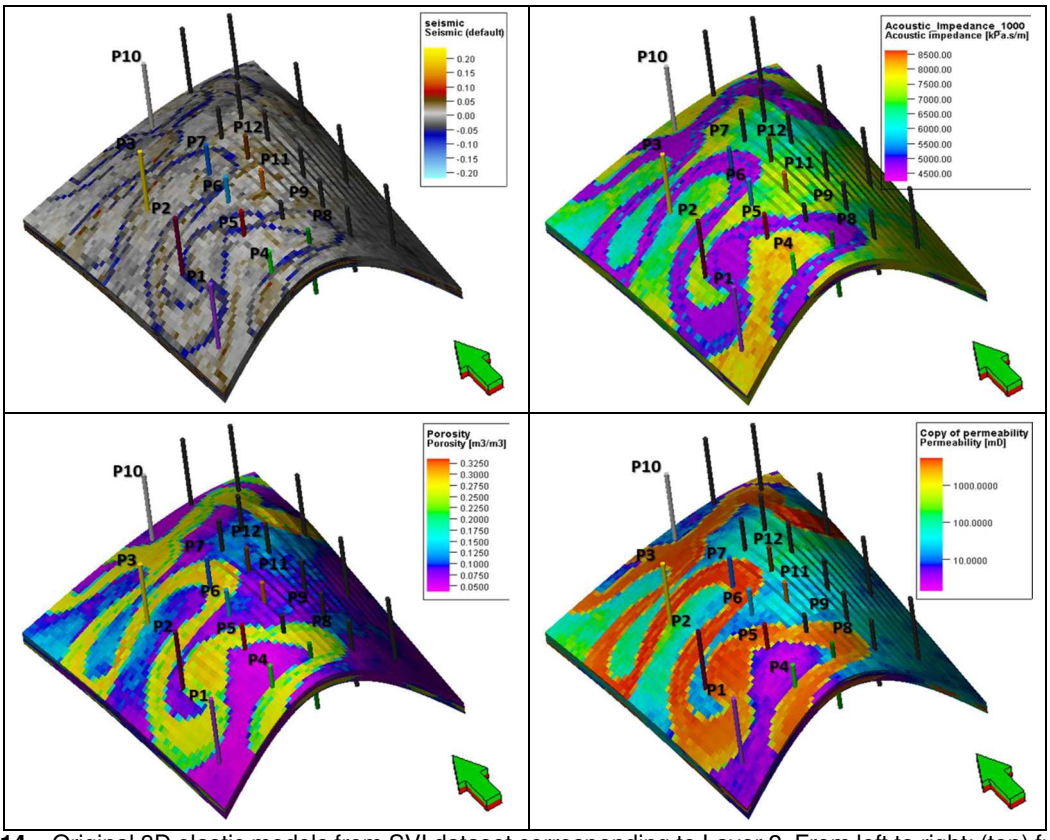

Figure 14 – Original 3D elastic models from SVI dataset corresponding to Layer 2. From left to right: (top) full-stack seismic and acoustic impedance model; (bottom) porosity and permeability models.

The option of choosing a meandering channels case is due to its complexity and difficulty for morphological reproduction in conventional geostatistical history matching. Since the properties such as porosity and permeability in sedimentary environments as sand channels tend to follow the pattern of the sediment deposition, i.e. the channels morphology. Furthermore, this non-stationary sedimentary environment represents a challenge because it has a high variability in terms of the spatial distributions of the sedimentary bodies and the shape and thickness of the many meandering channels vary considerably across the real petro-elastic models (Figure 15).

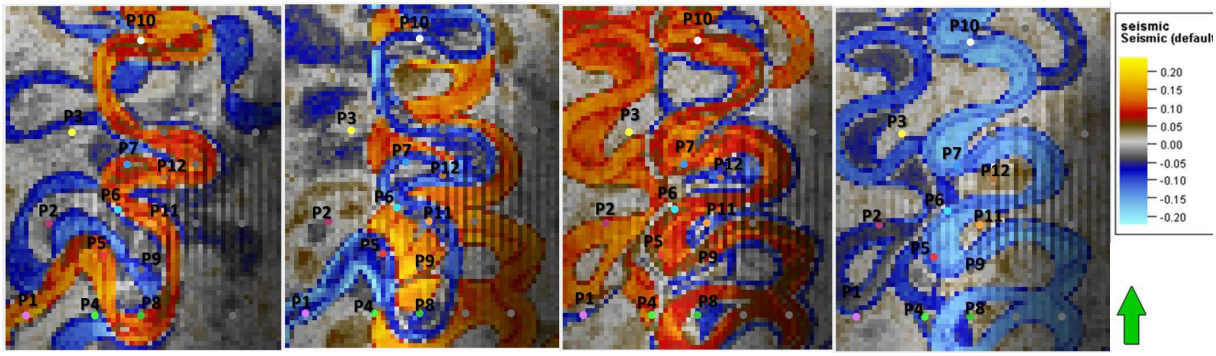

Figure 15 – High variability in terms of shape and thickness of the horizontal seismic sections extracted from the real full-stack seismic volume at different depths.

The conditioning data in this case study is the seismic data, the well logs: acoustic impedance, porosity and permeability (Figure 16); and the production data from each well: bottom hole pressure and water production rate.

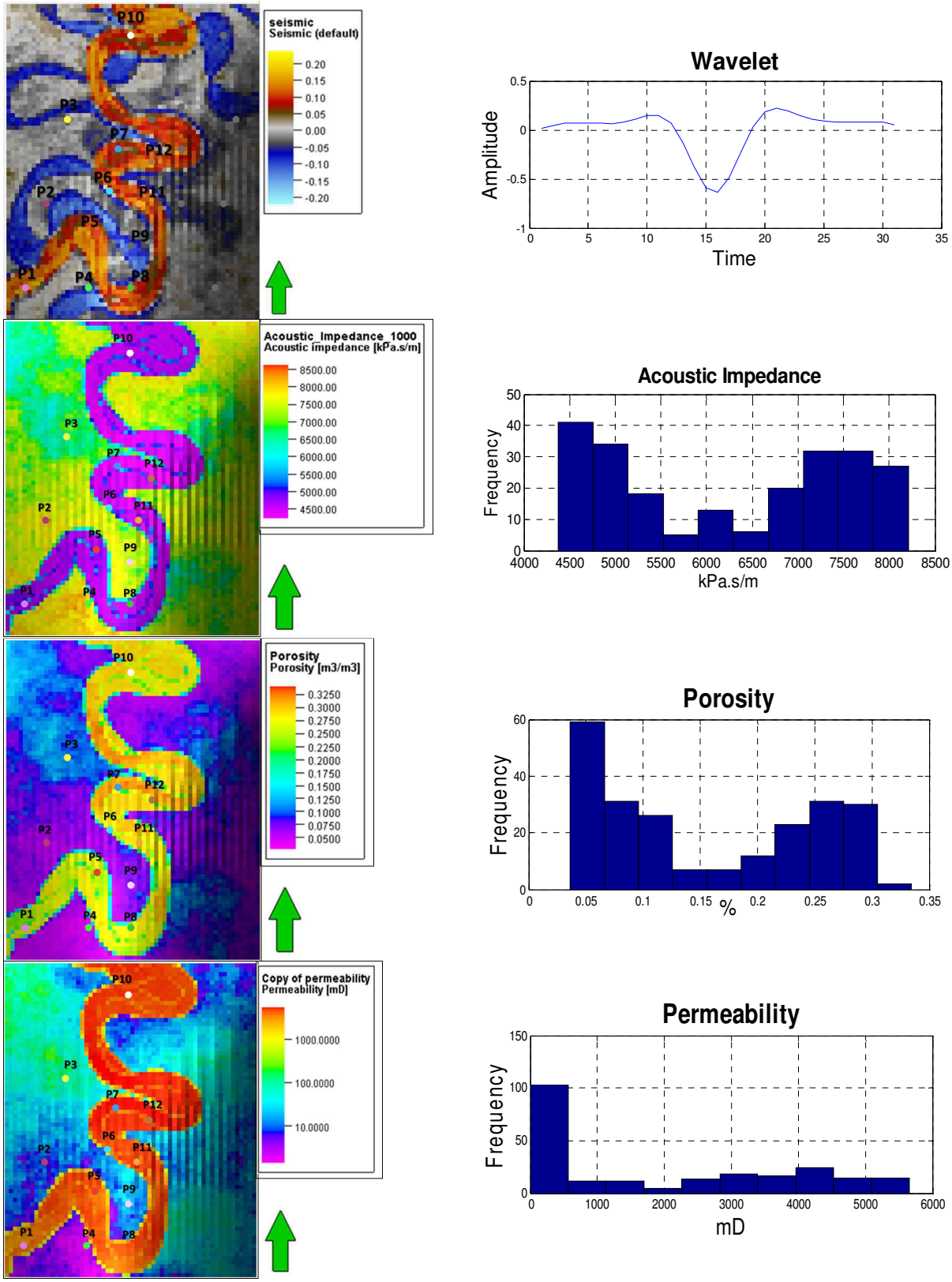

Figure 16 – From top to bottom: Seismic data, acoustic impedance, porosity and permeability horizontal slices, with wavelet and well-log data histograms, respectively.

The spatial continuity is defined by variogram model adjusted for the experimental variogram of each variable. The spatial continuity pattern of each property was modeled with an omnidirectional horizontal variogram with a range of about 700 meters and a vertical variogram range of 13 meters. The theoretical variogram used to model both directions was the spherical model and were computed using exclusively the set of conditioning well data (Figure 17).

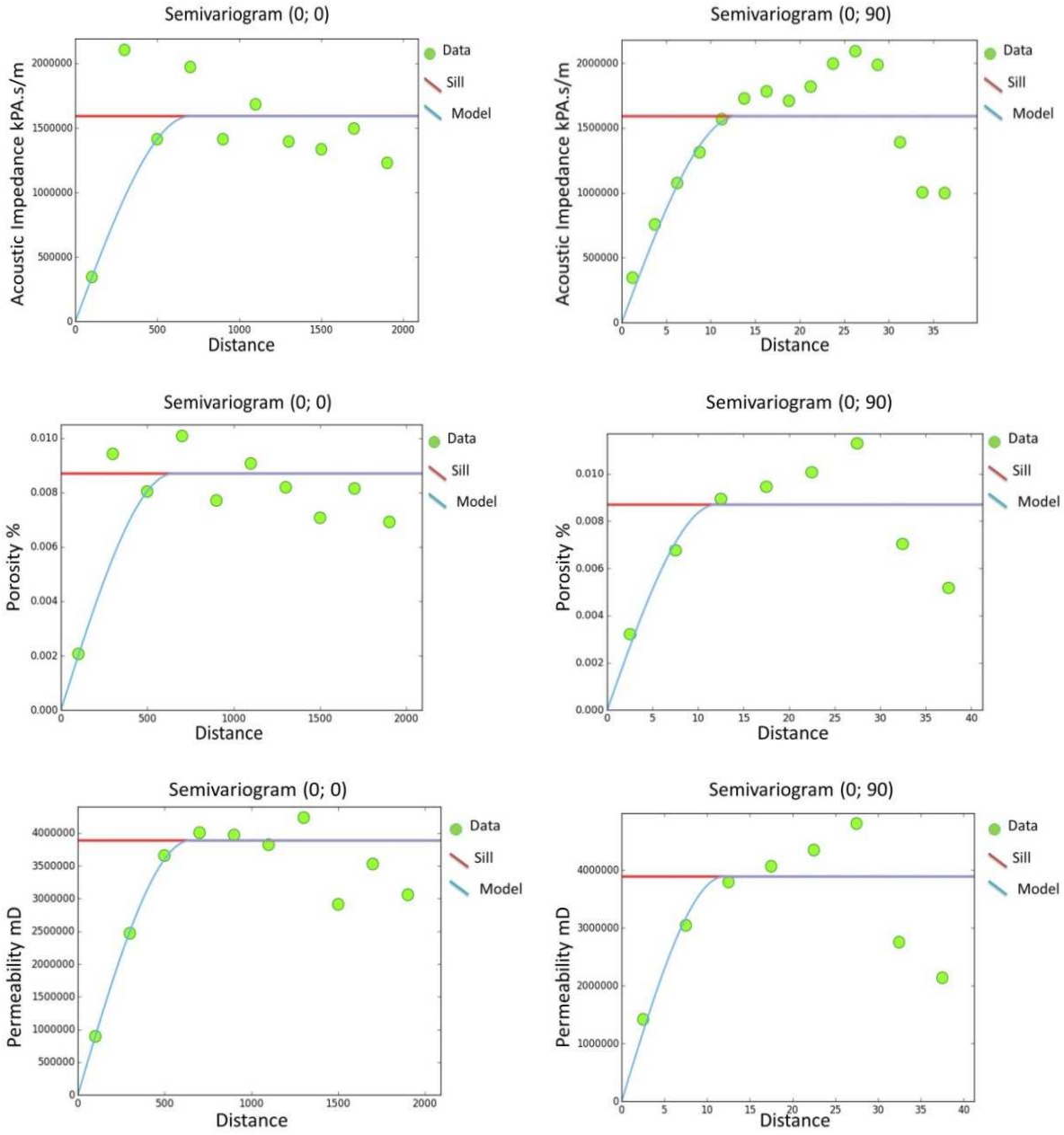

Figure 17 – Experimental (green circles) and modeled experimental variograms (blue line) for the omnidirectional (on the left) and vertical direction (on the right). From top to bottom: acoustic impedance, porosity and permeability.

The joint distributions of the well-log data for acoustic impedance versus porosity and porosity versus permeability are shown in (Figure 18).

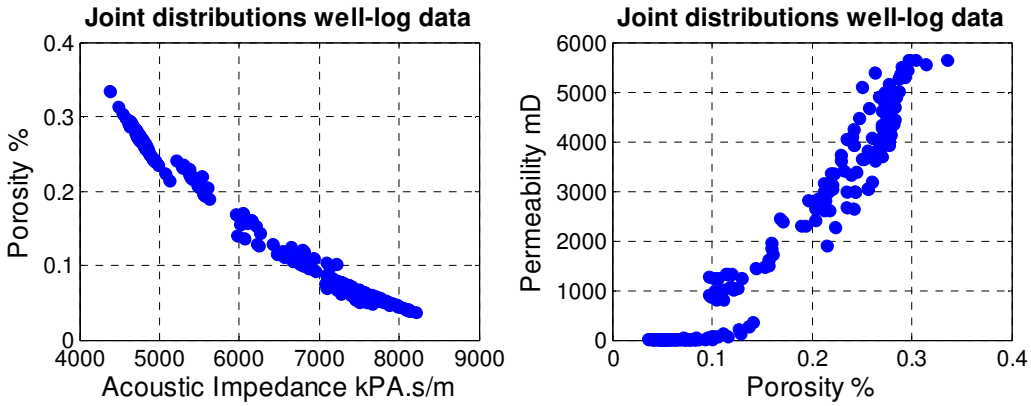

Figure 18 – Joint distributions from well-log data: (left) acoustic impedance versus porosity; and (right) porosity versus permeability.

The fluid flow simulator, Eclipse® 100 Black Oil (Schlumberger) ran over the original petrophysical models to produce the historic data used for the history matching problem. The reservoir was in production during approximately 3 years, from February 1st, 1975 until December 15th, 1977. The simulation target was the bottom hole pressure (BHP) at each well individually, which were shut after reaching a minimum BHP value, and the water production rate (WPR) at each well during the same period, due to the aquifer existence with constant flux. The oil production rate (OPR) constraint for this purpose was set for each well individually as constant.

The field has only 12 production wells, located preferentially in the Western part of the model (Figure 13) and the production start is due to the existent pressure supported by the aquifer. The schedule of production for the 12 wells start producing was different and the control data from the production wells was given by:

Table 1 - Wells production schedule and control data from the production wells: constant oil rate (OPR) and bottom hole pressure target (BHP).

Wells	Production Schedule	Oil Rate (OPR) stb/day	Bottom hole pressure (BHP) **Target** psi
P1	January 1st, 1975	100	4500
P2	January 1st, 1975	150	4000
P3	January 1st, 1975	150	3500
P4	November 1st, 1975	250	1000
P5	November 1st, 1975	250	1000
P6	November 1st, 1975	250	1000
P7	November 1st, 1975	250	1000
P8	March 1st, 1976	300	1000
P9	March 1st, 1976	300	1000
P10	March 1st, 1976	300	800
P11	July 1st, 1976	350	500
P12	July 1st, 1976	350	500

The historic production profiles for all the wells and variables of interest, bottom hole pressure (BHP) and water production rate (WPR) per well are shown next (Figure 19 and Figure 20).

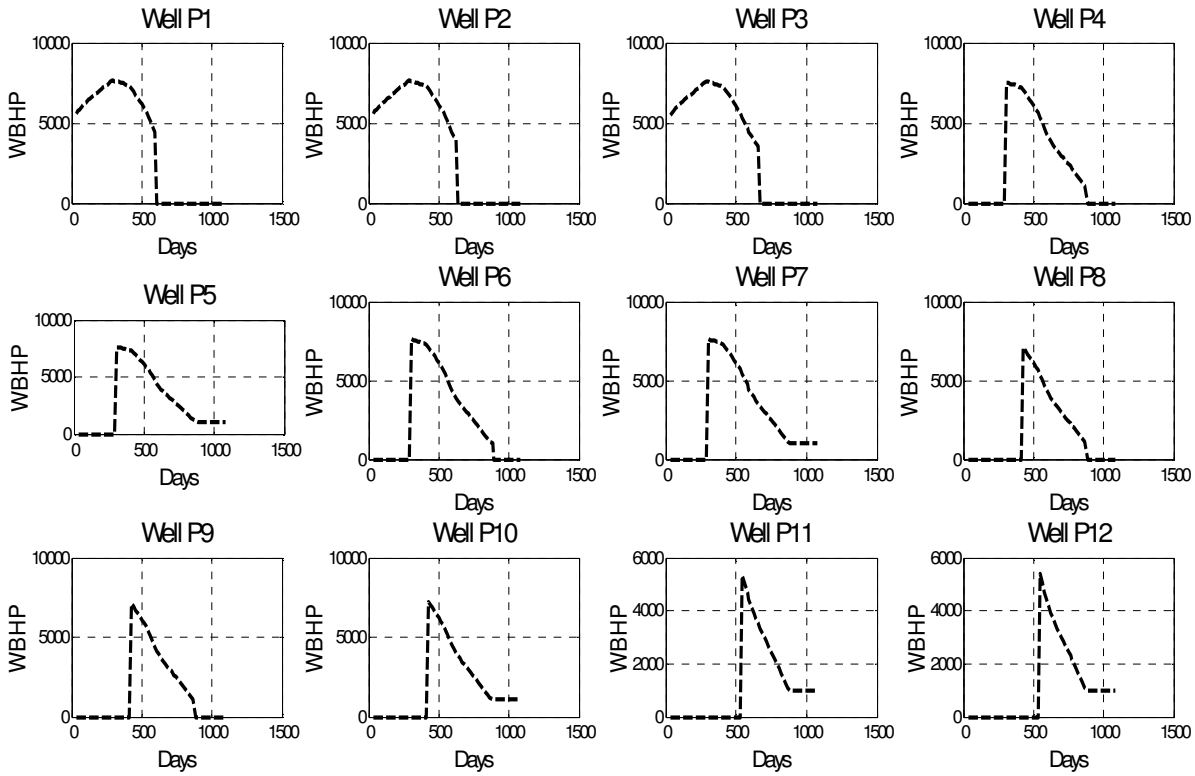

Figure 19 – Historic bottom hole pressure (WBHP) profiles for each well individually during the 3 years production.

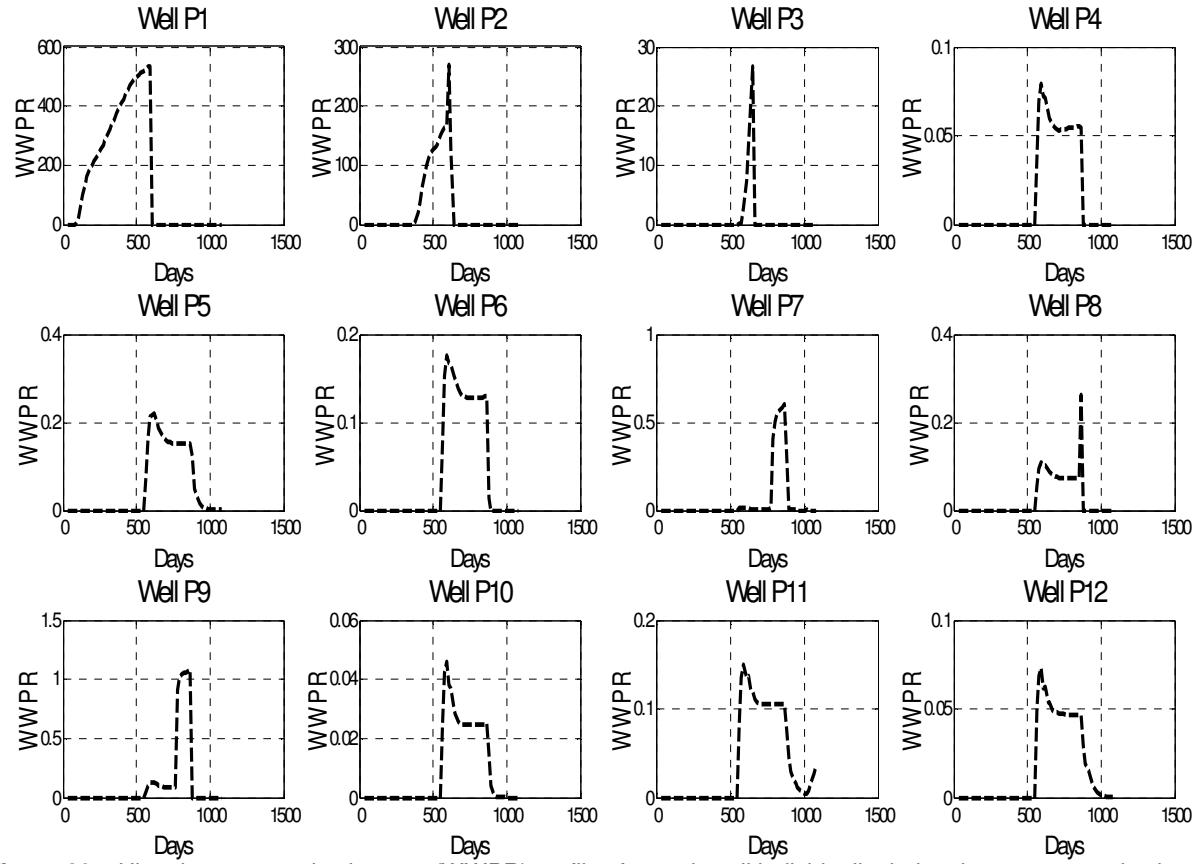

Figure 20 – Historic water production rate (WWPR) profiles for each well individually during the 3 years production.

4.2. Results

The proposed methodology attempts to solve simultaneously two different nonlinear inverse problems: history matching and seismic inversion through a single geostatistical iterative procedure aiming the convergence of petro-elastic models towards the real subsurface geology.

The results presented in this section are divided into two parts, depending on the influence well criteria used: geometric criteria (Section 4.2.1) and according to the correlation coefficients between permeability in each grid point and deviation in each well (Section 4.2.2). Those areas, surrounding or far away from the wells location can have a huge impact within the proposed methodology, and each criteria is performed differently within the geostatistical history matching with seismic data integration (Chapter 3) in order to assess the stability of the proposed methodology to the regionalization model.

4.2.1. Geometric Criteria

The definition of areas of influence for each well can have a significant impact on the convergence of the methodology since the convergence of the methodology inside those areas depends on the match towards the historical production and seismic reflection data simultaneously, which is measured recurring to MDS. By considering its definition according to a radius of influence, the areas outside the areas of influence of each well are only conditioned to the seismic inversion, i.e. the convergence of those areas are only conditioned to the seismic inversion and the areas inside those areas are simultaneously conditioned to both data. Thus, different radius for the area of influence for each well may generate considerable different inverted petro-elastic models of acoustic impedance, porosity and permeability (Figure 21, Figure 22 and Figure 23) while the convergence in terms of simulated and true production profiles for each well individually is reached (Figure 24 and Figure 25). Two different radius size were tested, a larger with 10 cells dimensions and a smaller one of 5 cells. An acceptable convergence was reached after 10 iterations with 16 ensembles of petro-elastic models generated per iteration.

The inverted petro-elastic models, acoustic impedance, porosity and permeability (Figure 21 to Figure 23) match considerably well the real ones in reproducing the main geological features of interest. In the first iteration they are only conditioned to the available well-log data and consequently the meandering structures are not reproduce. However, after the first iteration, the inverted petro-elastic models start to be conditioned simultaneously to the real seismic and historic production data improving the reproduction of the main sedimentary features.

Different sizes of the area of influence of each well has different impact on the resulting inverted petro-elastic models: smaller influence areas allow the reproduction with more accuracy and detail of the high variability of the real petro-elastic models, i.e. the small and large scale non-stationary patterns; while in other hand, (on the top of the figures) higher well size influence definition are only able to reproduce the main features, the large scale non-stationary patterns. Therefore reflecting the importance of the seismic reflection data as part of the iterative geostatistical procedure.

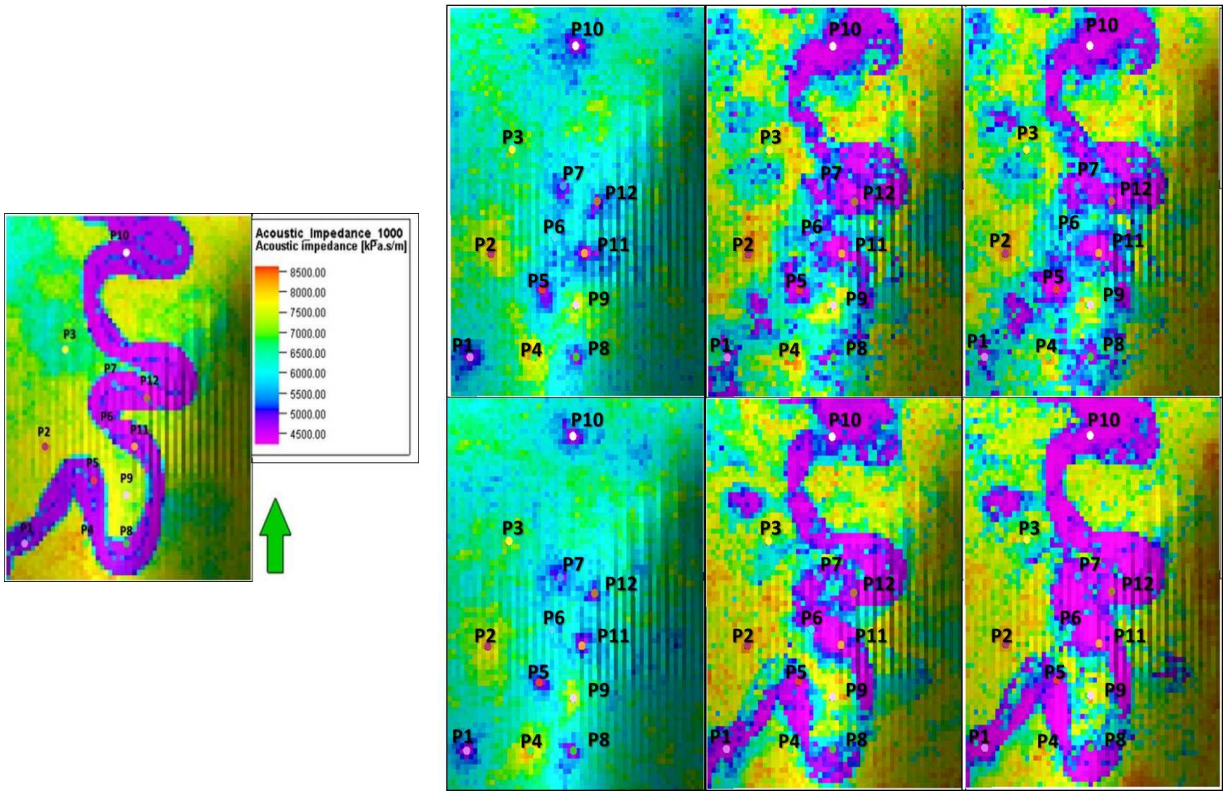

Figure 21 – Horizontal sections extracted from (on the left) the real acoustic impedance model and (on the right) the mean of the acoustic impedance models simulate (top) for the larger influence zone around each well and (bottom) for the smaller area of influence around each well: (from left to right) iteration 1; iteration 5; and iteration 10. The horizontal sections are at the same depth as the ones shown in Figure 16.

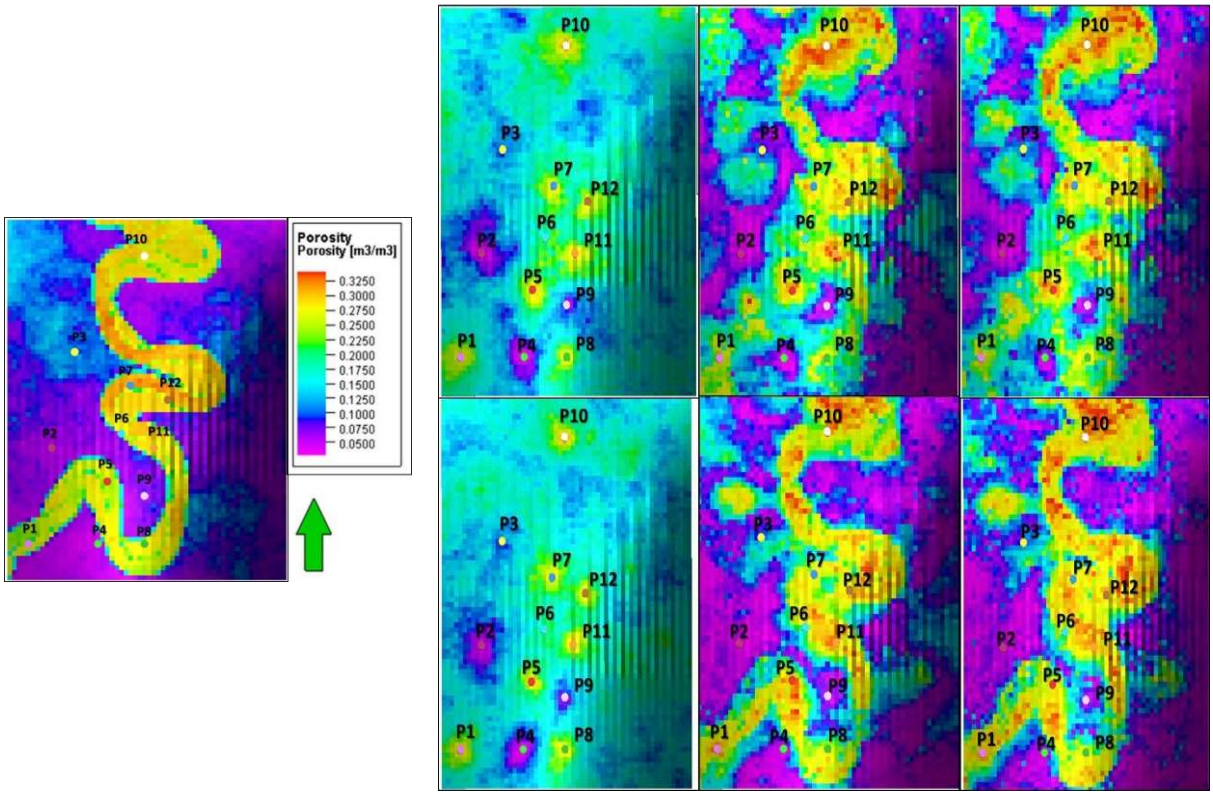

Figure 22 – Horizontal sections extracted from (on the left) the real porosity model and (on the right) the mean of the porosity models simulate (top) for the higher well size influence and (bottom) for the small well size influence at: (from left to right) iteration 1; iteration 5; and iteration 10. The horizontal sections are at the same depth as the ones shown in Figure 16.

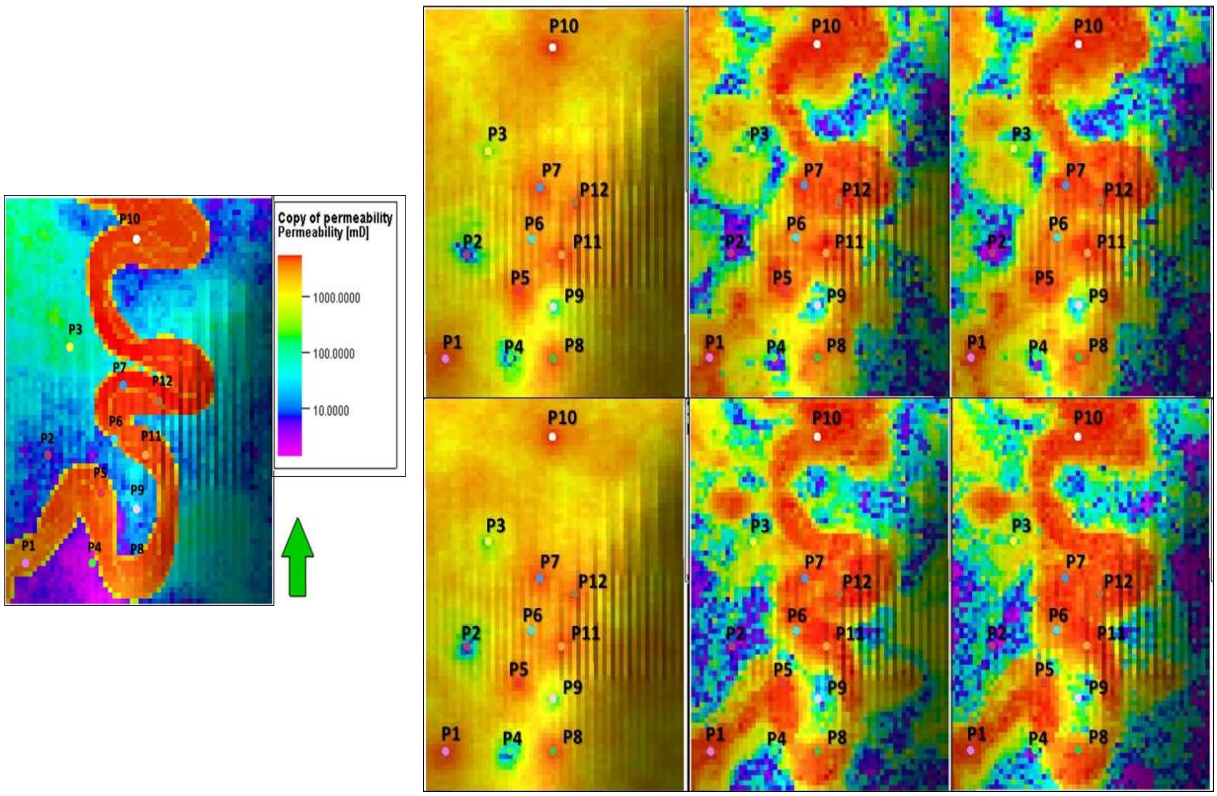

Figure 23 – Horizontal sections extracted from (on the left) the real permeability model and (on the right) the mean of the permeability models simulate (top) for the higher well size influence and (bottom) for the small well size influence at: (from left to right) iteration 1; iteration 5; and iteration 10.The horizontal sections are at the same depth as the ones shown in Figure 16.

Along with the inverted petro-elastic models, it is possible to retrieve the production responses for each of the model simulated during the entire iterative geostatistical procedure. The production profiles obtained through fluid flow simulation uses as input the inverted permeability and porosity models and shows its convergence from the first iteration until the last iteration. However, besides being performed with different well size influence parameterization, the match towards the historic production data have similar convergence for the parameters taken into account for each one of the 12 wells: bottom hole pressure (BHP) and water production rate (WPR), as the Figure 24 and Figure 25 shows.

The 12 producers wells shows a very good convergence in terms of bottom hole pressure (BHP), taking into account the assumed deviation of 10% regarding the real historic production data. In other hand, in terms of water production rate (WPR) the convergence is not homogeneous in the 12 producers wells since while the P1, P4 shows a good convergence and P9, P10 a reasonable convergence, the other wells are not able to reproduce the historical production at all which may be related with the porous connectivity or with the implemented production strategy because the only water produced is related to the aquifer action, making the water production rate a good parameter to match but a challenging task.

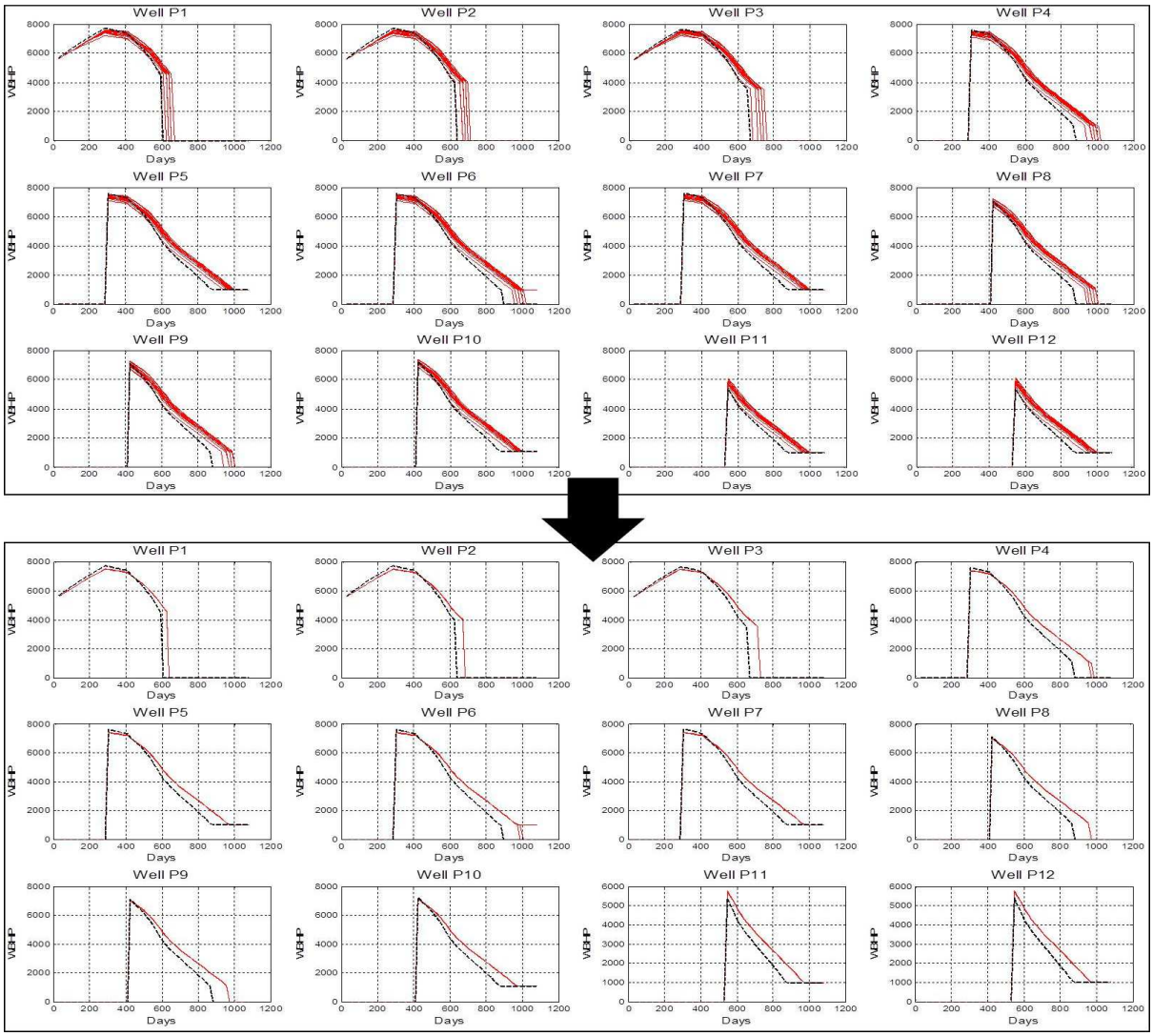

Figure 24 – Bottom hole pressure profiles convergence, form the first iteration at the last iteration (10), for each well individually during the 3 years production. Back dashed curve corresponds to the historic production data. The red thick line corresponds to the response of the 16 inverted models of the first and last iteration.

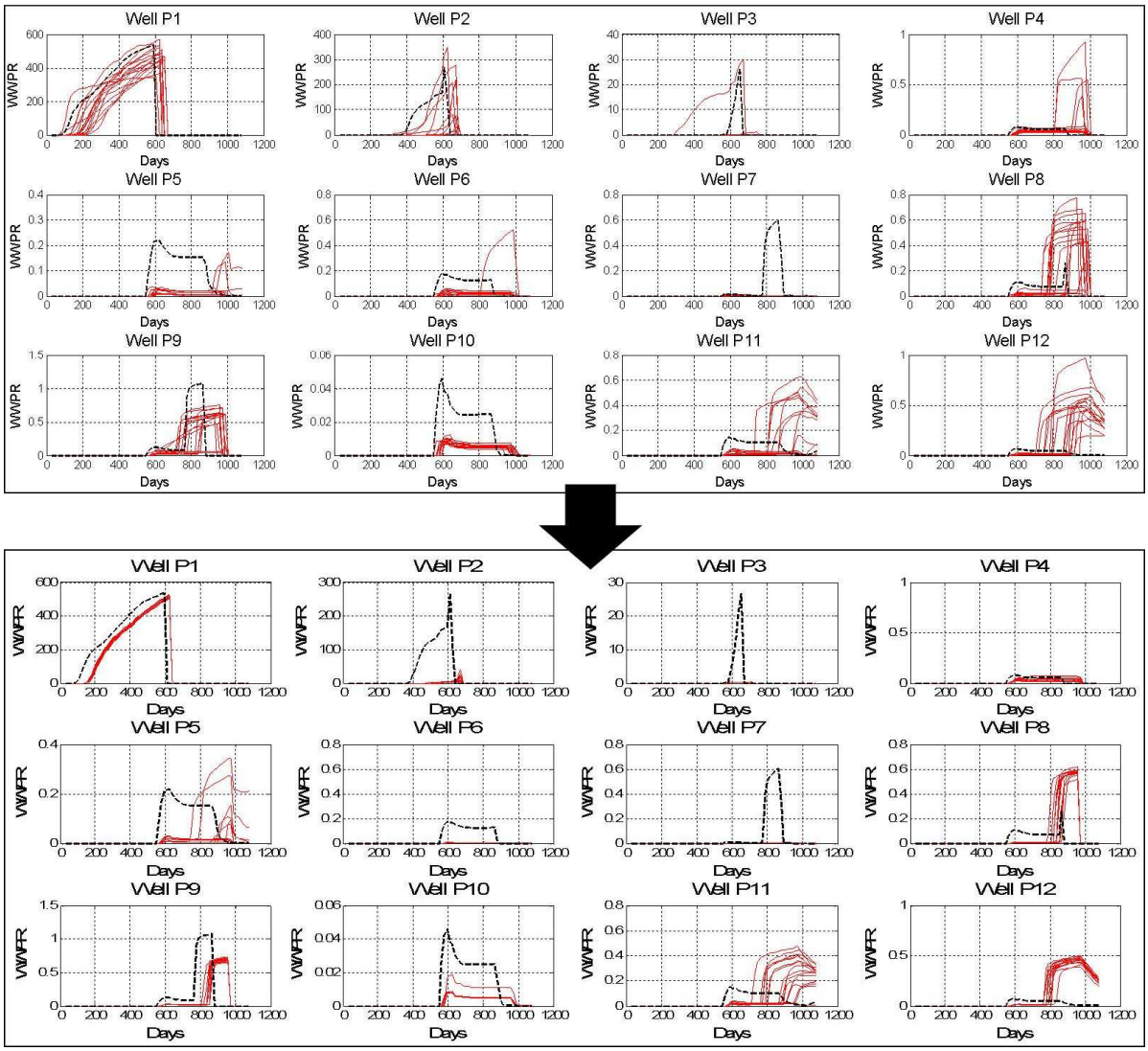

Figure 25 – Water production rate profiles convergence, form the first iteration at the last iteration (10), for each well individually during the 3 years production. Back dashed curve corresponds to the historic production data. The red thick line corresponds to the response of the 16 inverted models of the first and last iteration.

The resulting synthetic seismic volume are able to reproduce approximately the non-stationary patterns related with the meandering channels reproducing its high variability in terms of shape and thickness (Figure 26).

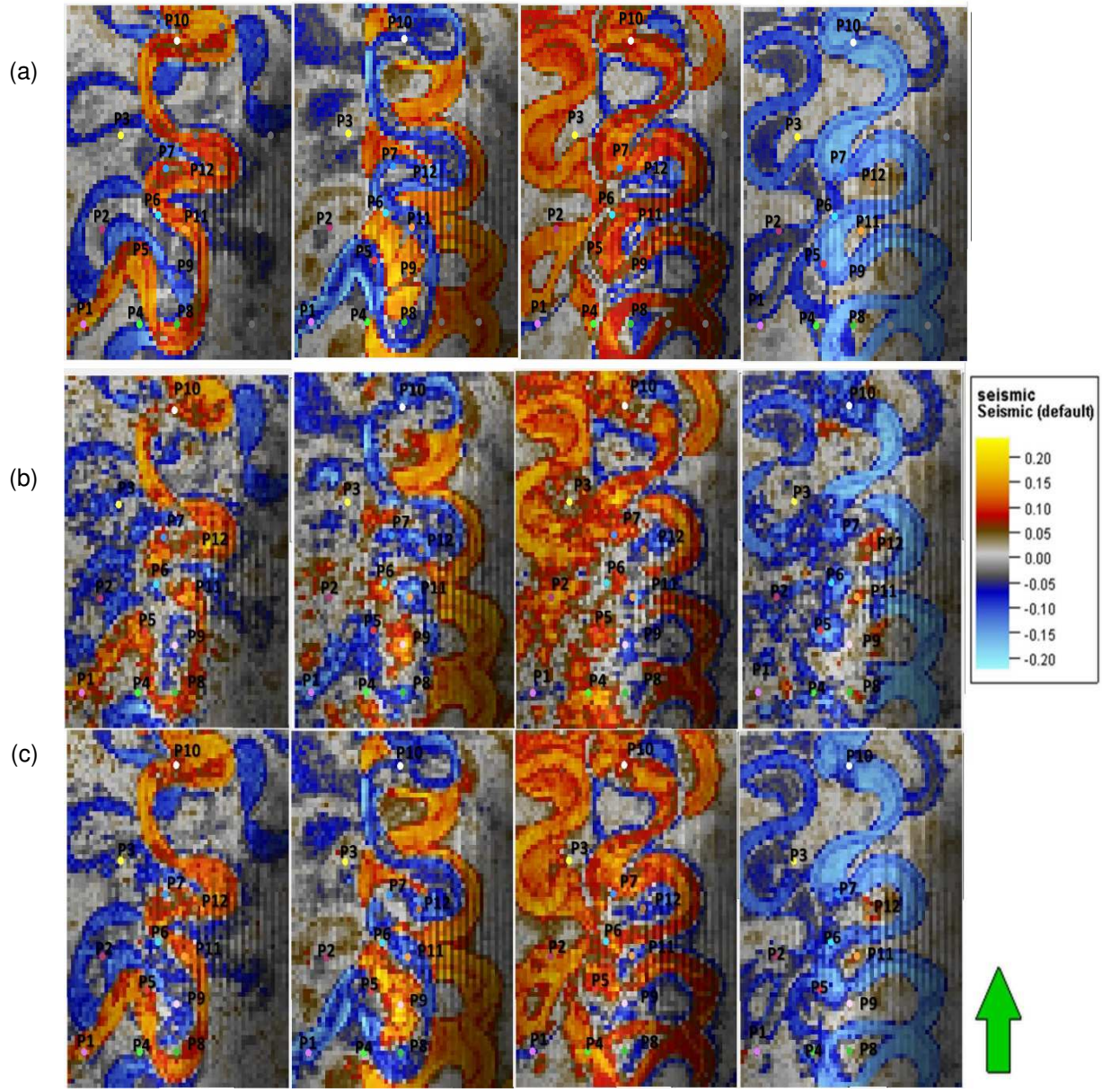

Figure 26 – Horizontal sections extracted from (a) the real seismic data, (b and c) the synthetic seismic at the end of the iterative geostatistical process for the higher and smaller areas of influence for each well at different depths.

The method with smaller areas of influence (case b, Figure 26) is more continuous and accurate in reproducing the both non-stationary patterns.

Since this thesis aims to solve simultaneously two different non-linear inverse problems, through the best local correlation cube created at the end of each iteration it is possible to interpret the evolution of the convergence methodology by visually inspecting the best local correlation coefficients volumes computed at the end of each iteration (Figure 27).

At the end of the first iteration the convergence is lower within the defined area of influence when compared with the rest of the reservoir. The petro-elastic models selected to compose the best models

are constrained to the match towards the historic production and seismic data simultaneously. Due to this reason, it is not possible to guarantee that those models will converge towards the observed seismic data, however, in areas outside of the defined well influence the petro-elastic models selected to compose the best local models ensure the highest correlation coefficient between synthetic and real seismic.

As long as the iterative geostatistical procedure continues, the convergence of the models that best match the historic production and seismic data simultaneously starts to be achieved within the defined well influence in terms of correlation coefficient, essentially due to the convergence outside those areas were the convergence of the petro-elastic models are only constrained by the seismic data. The convergence of the petro-elastic models that best match towards the historic production data and the seismic data is evident in terms of correlation coefficient, from iteration 1 to iteration 10.

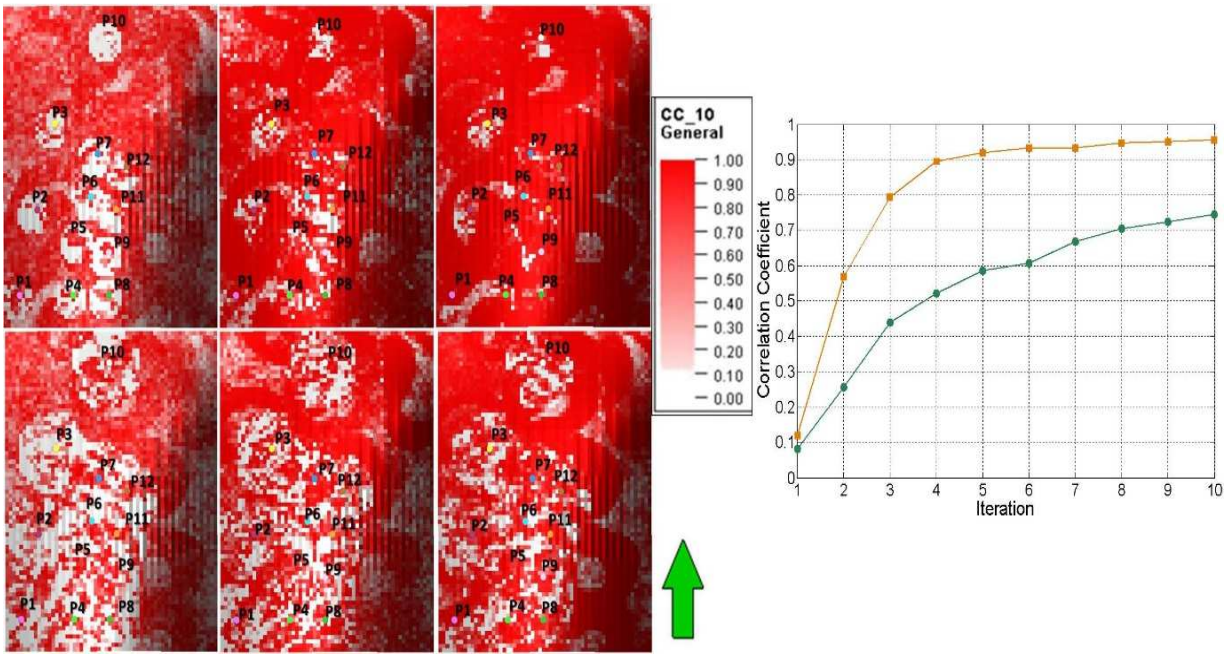

Figure 27 – Horizontal sections extracted from the best local correlation volume (top) for the smaller well size influence and (bottom) for the higher well size influence at the end of: (from left to right) iteration 1; iteration 5; and iteration10. And on the right, the correlation coefficient evolution for each one, were the green curve refers to the higher area of influence of each well size and the orange curve corresponds to the smaller area of influence for each well.

As a geostatistical inverse methodology, the inverted petro-elastic models simulated during the entire procedure must reproduce the marginal distributions for acoustic impedance, porosity and permeability, as estimated from the experimental data (Figure 28) as well as the joint distributions between acoustic impedance versus porosity and porosity versus permeability (Figure 29).

The reproduction of the spatial continuity pattern in all the inverted petro-elastic models is ensured by using stochastic sequential simulation and co-simulation algorithms. Therefore, the spatial continuity pattern imposed by a variograma models estimated from the 12 wells (Figure 17) are also reproduced in all the petro-elastic models simulated during the iterative inversion methodology (Figure 30).

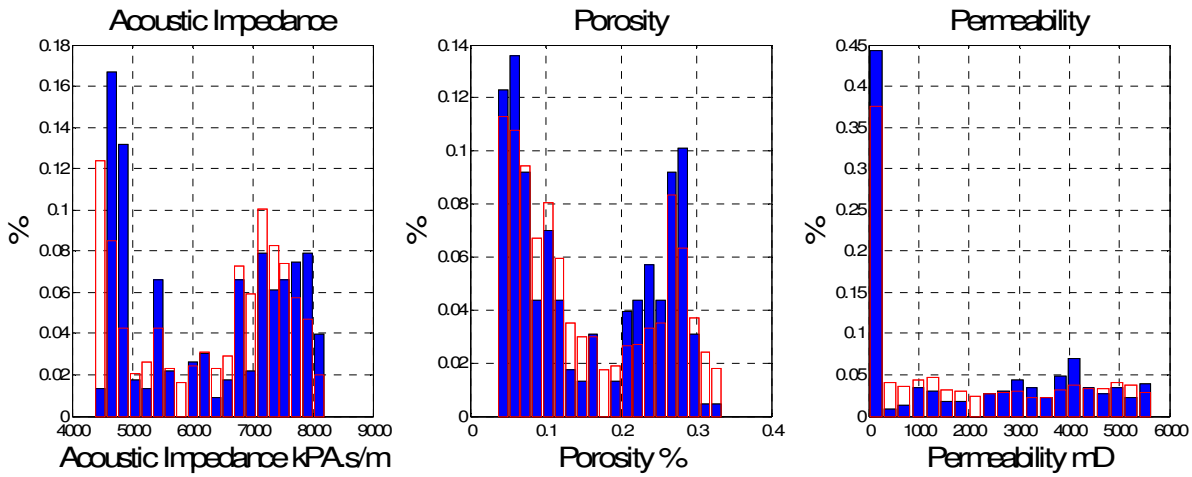

Figure 28 – Comparison between the marginal distributions of acoustic impedance, porosity and permeability estimated from the well-log data (in red) and those retrieved from the last elastic inverted model from the last iteration (blue filled bars).

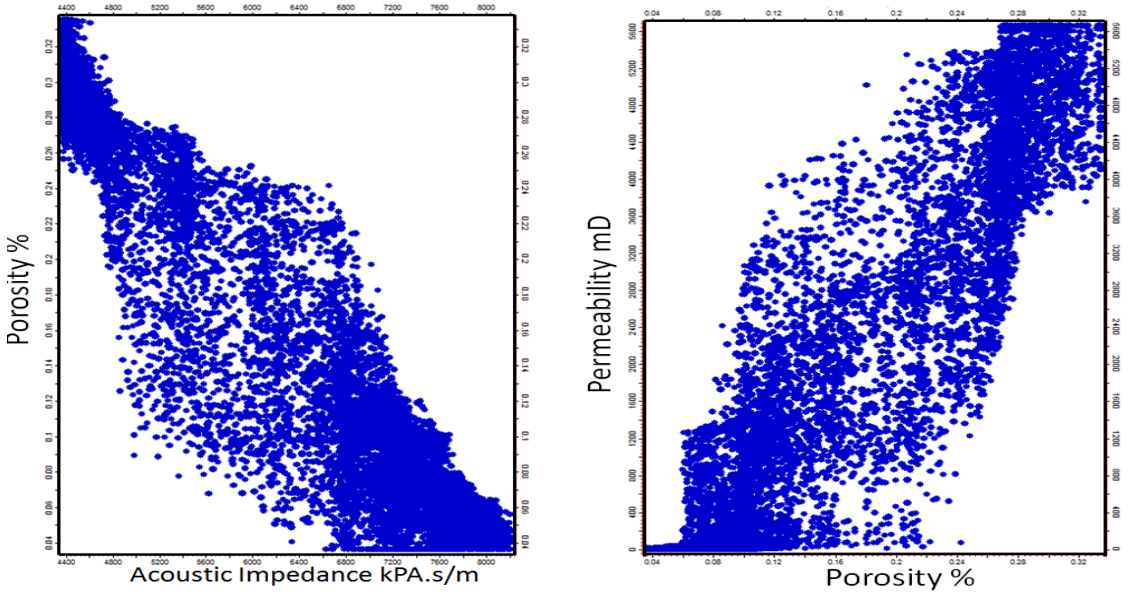

Figure 29 – Joint distributions estimated from the last elastic inverted model from the last iteration: (on the left) acoustic impedance versus porosity and (on the right) porosity versus permeability. They reproduce the joint distributions estimated from the well-log data.

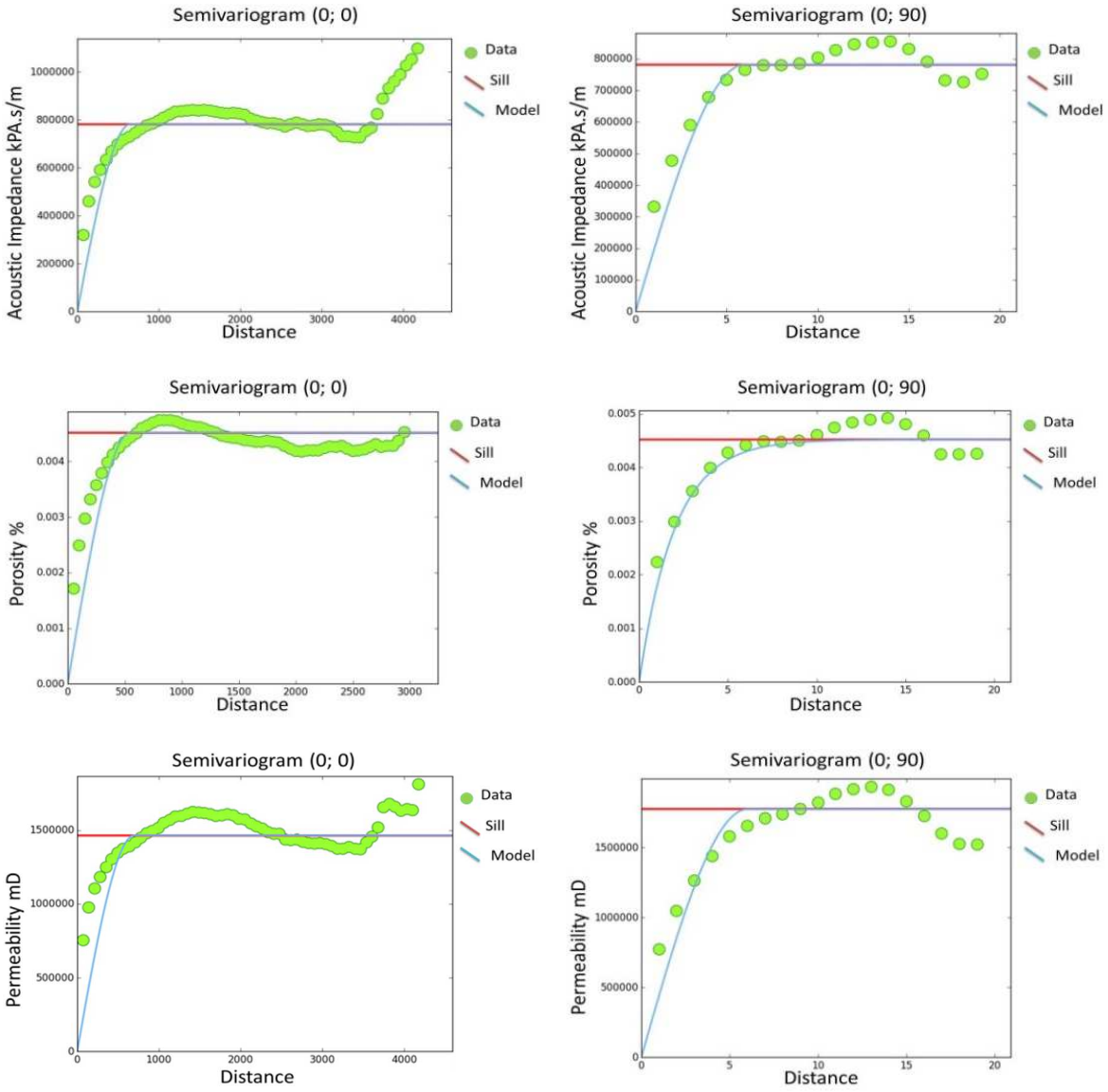

Figure 30 – Experimental (green circles) and modeled variograms (blue line) for the omnidirectional (on the left) and vertical directions (on the right) for: (from top to bottom) acoustic impedance, porosity and permeability. The variograms were computed over one grid model of the sixth iteration (compare with Figure 17).

4.2.2. <u>According to correlation coefficients between permeability in each grid point and deviation in each well</u>

Due to the non-uniqueness nature of the history matching problems ensuring a small deviation over the production profiles, it does not ensure how the retrieved petrophysical models are close to the real solution.

The definition of well influence according to correlation coefficients between permeability in each grid node and the deviations between the simulated and real historic production data in each one of the wells allows to constrain all grid cells to the match towards the historic production and the seismic reflection data simultaneously. The proposed methodology is highly dependent on the convergence of both data,

however this does not guarantee the reproduction of the main geological features of the inverted petro-elastic models, acoustic impedance, porosity and permeability (Figure 31, Figure 32 and Figure 33 respectively). Therefore, different dynamic and seismic weights were considered, i.e. increase or decrease the influence of the seismic reflection data within the iterative geostatistical procedure.

Notice that the convergence was reached after 6 iterations with 32 ensembles of petro-elastic models: acoustic impedance, porosity and permeability; which were simulated and co-simulated per iteration.

The inverted petro-elastic models, acoustic impedance, porosity and permeability (Figure 31 to Figure 33) match considerably the real ones, reproducing the main geological trends. In the first iteration they are only conditioned to the available well-log data and consequently the meandering structures are not reproduced. However, after the first iteration, the inverted petro-elastic models start to be conditioned to the real seismic and historic production data as well, which improves the reproduction of the main sedimentary features of the real petro-elastic models. Nevertheless, is also evident the difference between the iterative geostatistical procedure when the seismic have higher influence (on the bottom of the figures) where the spatial continuity and connectivity of the main features is reproduce instead the main geological trend (top of the figures). Thus, by considering higher influence of the seismic reflection data, as the iterative geostatistical procedure gradually increases its convergence the reproduction of the large and some of small scale non-stationary patterns is clearly.

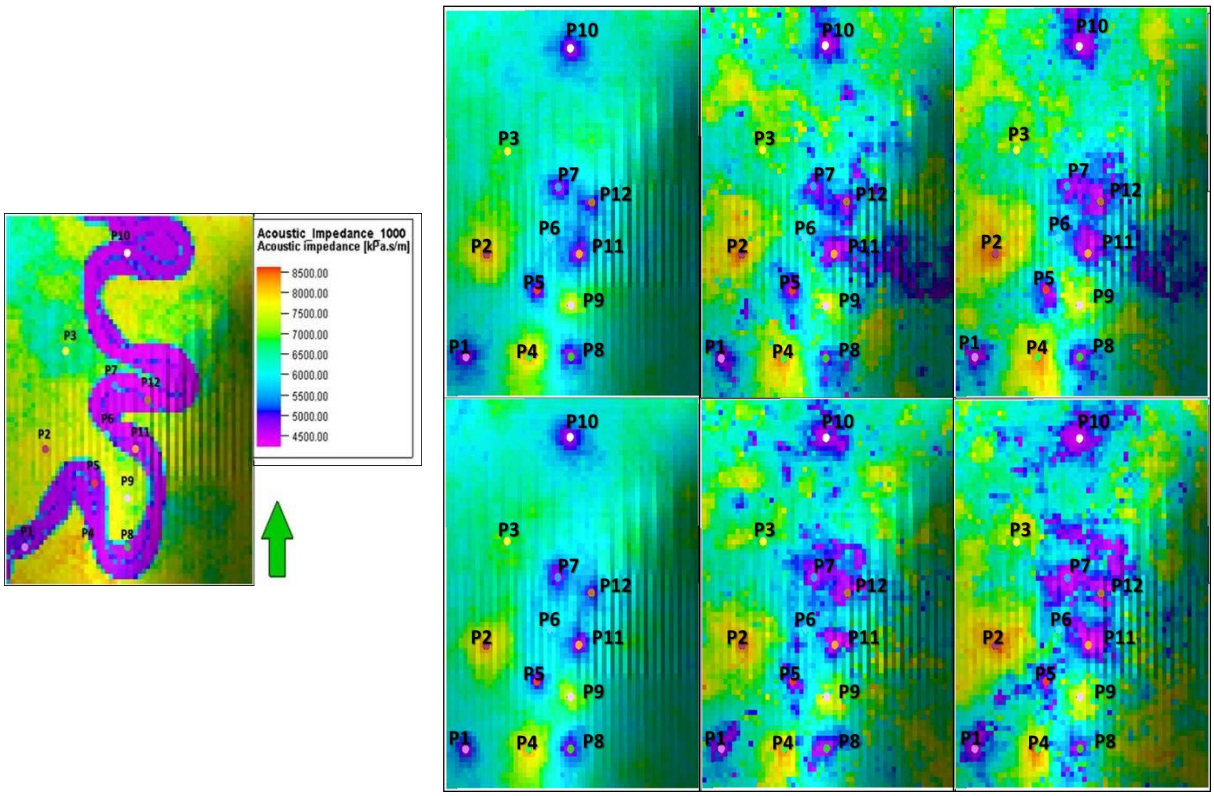

Figure 31 – Horizontal sections extracted from (on the left) the real acoustic impedance model and (on the right) the mean of the acoustic impedance models simulate (top) for the less seismic influence and (bottom) for the higher seismic influence at: (from left to right) iteration 1; iteration 3; and iteration 6 of the iterative geostatistical procedure. The horizontal sections are at the same depth as the ones shown in Figure 16.

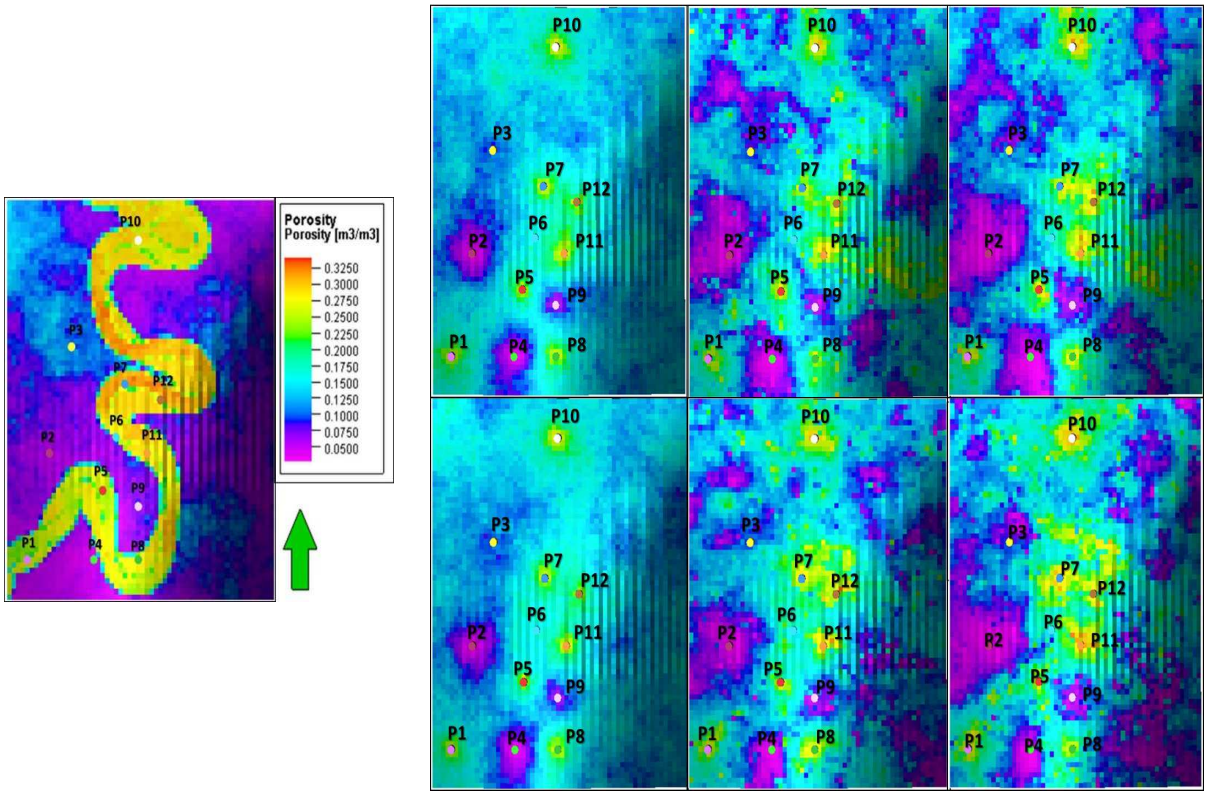

Figure 32 - Horizontal sections extracted from (on the left) the real porosity model and (on the right) the mean of the porosity models simulate (top) for the less seismic influence and (bottom) for the higher seismic influence at: (from left to right) iteration 1; iteration 3; and iteration 6 of the iterative geostatistical procedure. The horizontal sections are at the same depth as the ones shown in Figure 16.

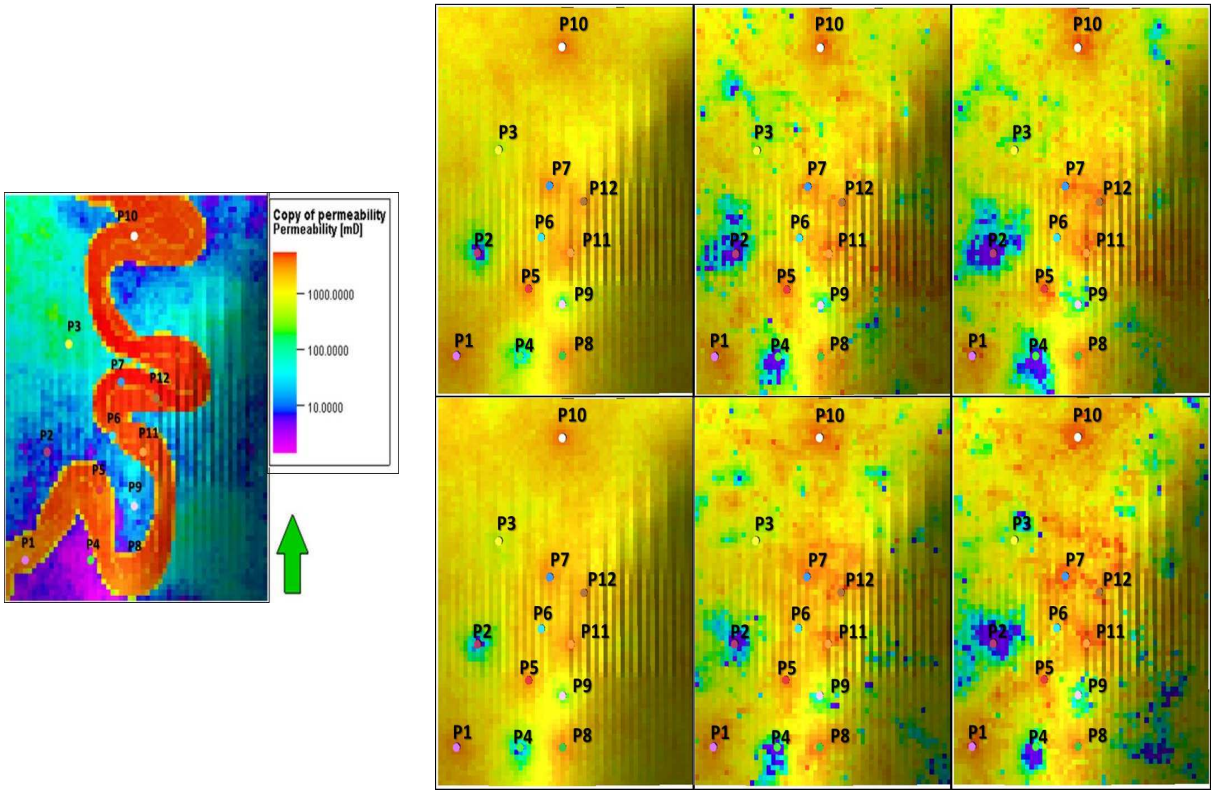

Figure 33 - Horizontal sections extracted from (on the left) the real permeability and (on the right) the mean of the permeability models simulate (top) for the less seismic influence and (bottom) for the higher seismic influence at: (from left to right) iteration 1; iteration 3; and iteration 6 of the iterative geostatistical procedure. The horizontal sections are at the same depth as the ones shown in Figure 16.

At the end the iterative geostatistical procedure, the synthetic seismic volume where it was considered the seismic higher weight is able to reproduce better the non-stationary patterns related with the meandering channels and its high variability in terms of shape and thickness (on the right of the Figure 34). In the other hand, when this influence is lower the synthetic seismic volume cannot reproduce so accurately the non-stationary patterns but only some proportions without continuity (on the middle of the Figure 34).

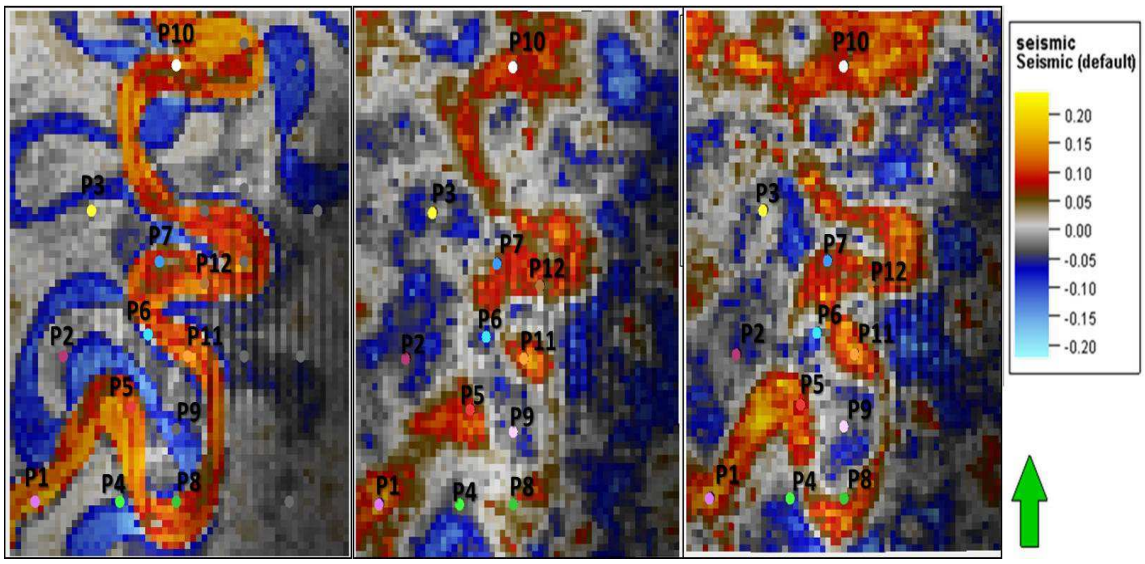

Figure 34 - Horizontal sections extracted from (left) the real seismic data, (middle) the synthetic seismic with less seismic weight and (right) the synthetic seismic with higher seismic weight at the end of the iterative geostatistical process at different depths.

Along with the inverted petro-elastic models, it is possible to retrieve the production responses for each of the model simulated during the entire iterative geostatistical procedure. The production profiles obtained through fluid flow simulation uses as input the inverted permeability and porosity models and shows its convergence from the first iteration until the last iteration

The match towards the historic production data convergence for the parameters taken into account for each one of the 12 wells: bottom hole pressure (BHP) and water production rate (WPR). Figure 35 and Figure 36 corresponds to the iterative geostatistical procedure with less seismic influence, reproducing naturally a better matching convergence; while Figure 37 and Figure 38 corresponds to the iterative geostatistical procedure with higher seismic influence, that despite not reproducing the match as good as in the previous one, shows good convergence along with the iterative procedure.

The difference between both methods in terms of water production rate (WPR) convergence is more evident when it is considered more or less dynamic influence within the process since more dynamic influence more convergence towards the real historic production data is achieved (Figure 35 and Figure 36).

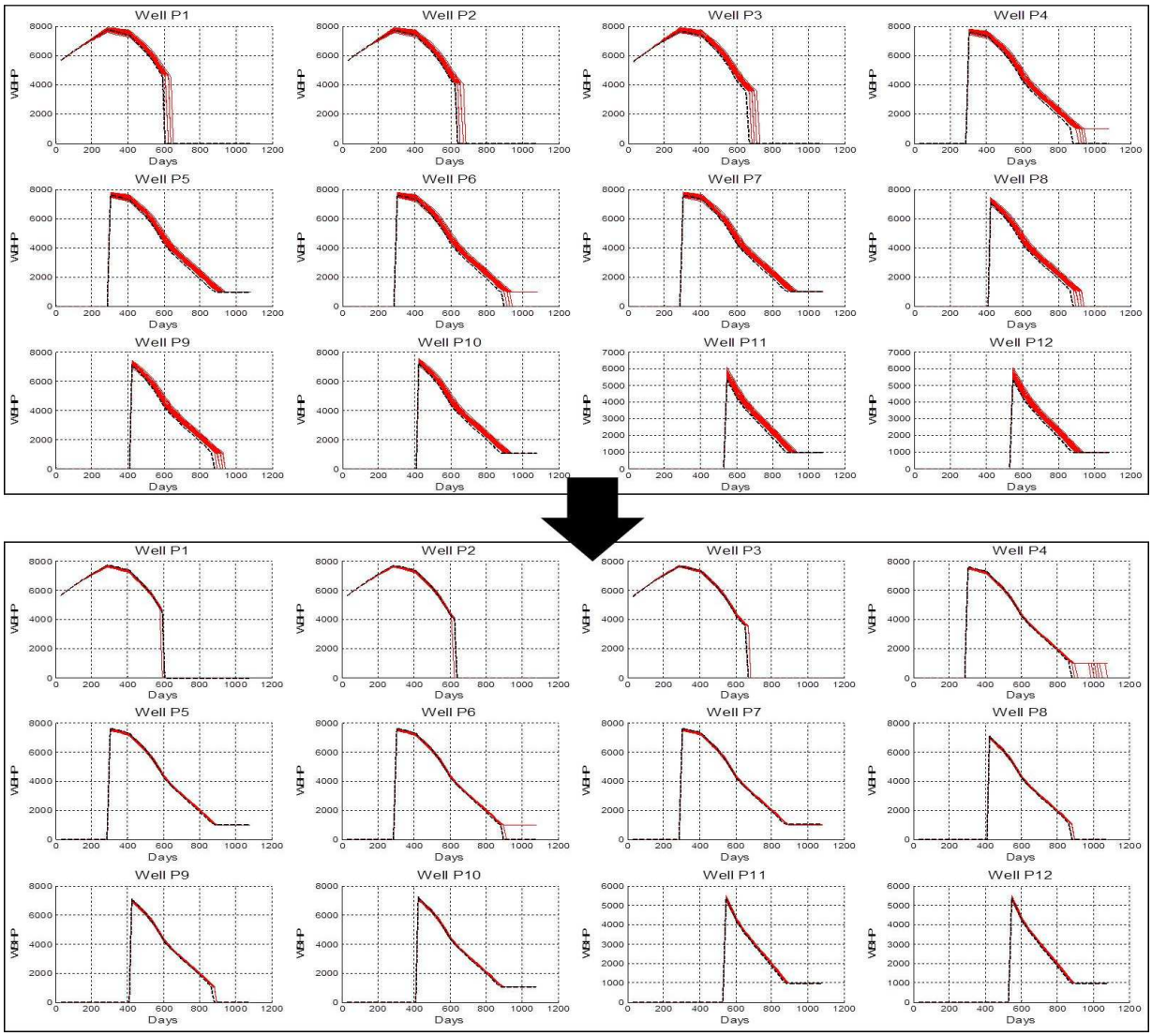

Figure 35 - Bottom hole pressure profiles convergence, form the first iteration at the last iteration (6), for each well individually during the 3 years production. Back dashed curve corresponds to the historic production data. The red thick line corresponds to the response of the 16 inverted models of the first and last iteration.

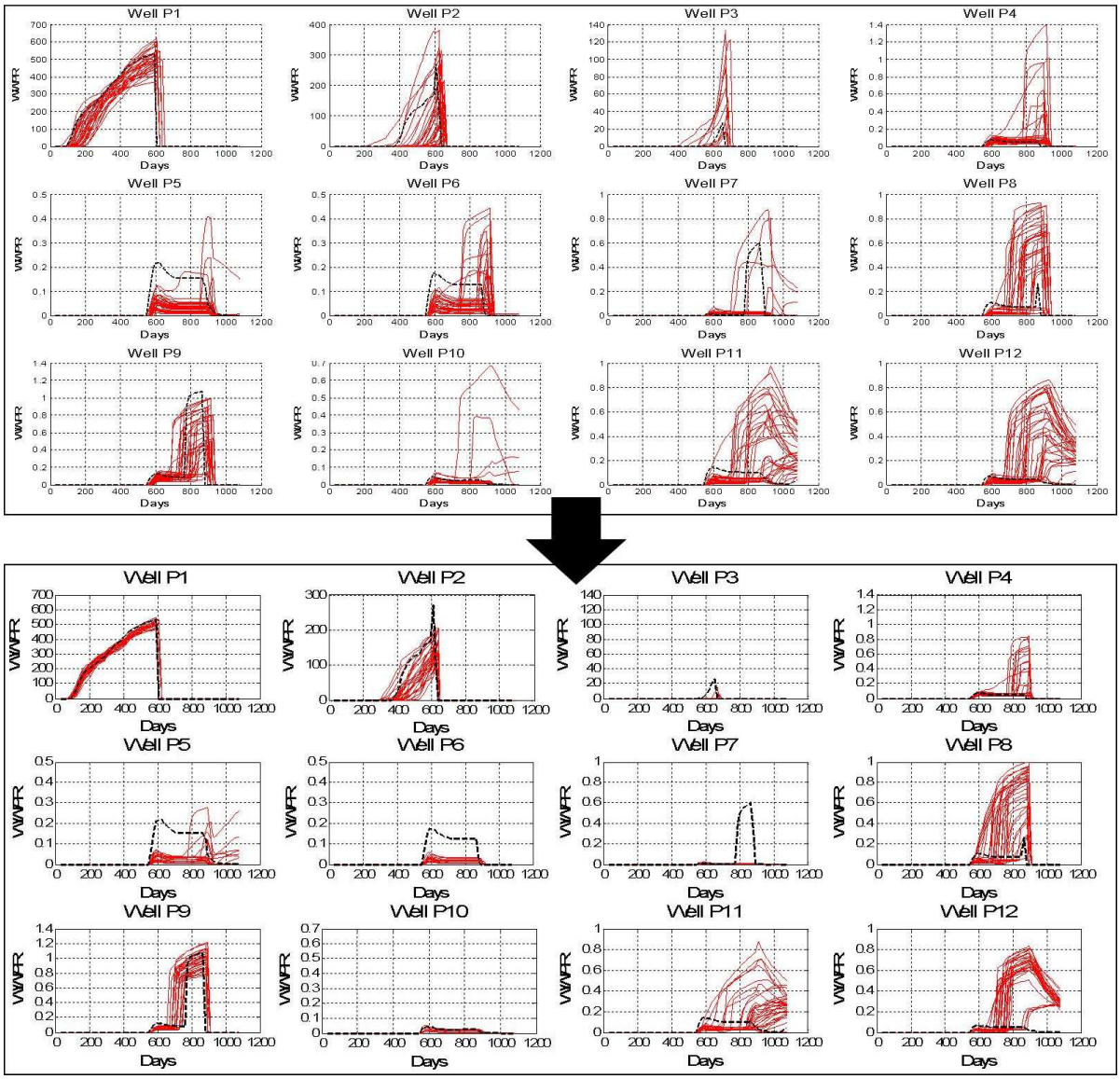

Figure 36 – Water production rate profiles convergence, form the first iteration at the last iteration (6), for each well individually during the 3 years production. Back dashed curve corresponds to the historic production data. The red thick line corresponds to the response of the 16 inverted models of the first and last iteration.

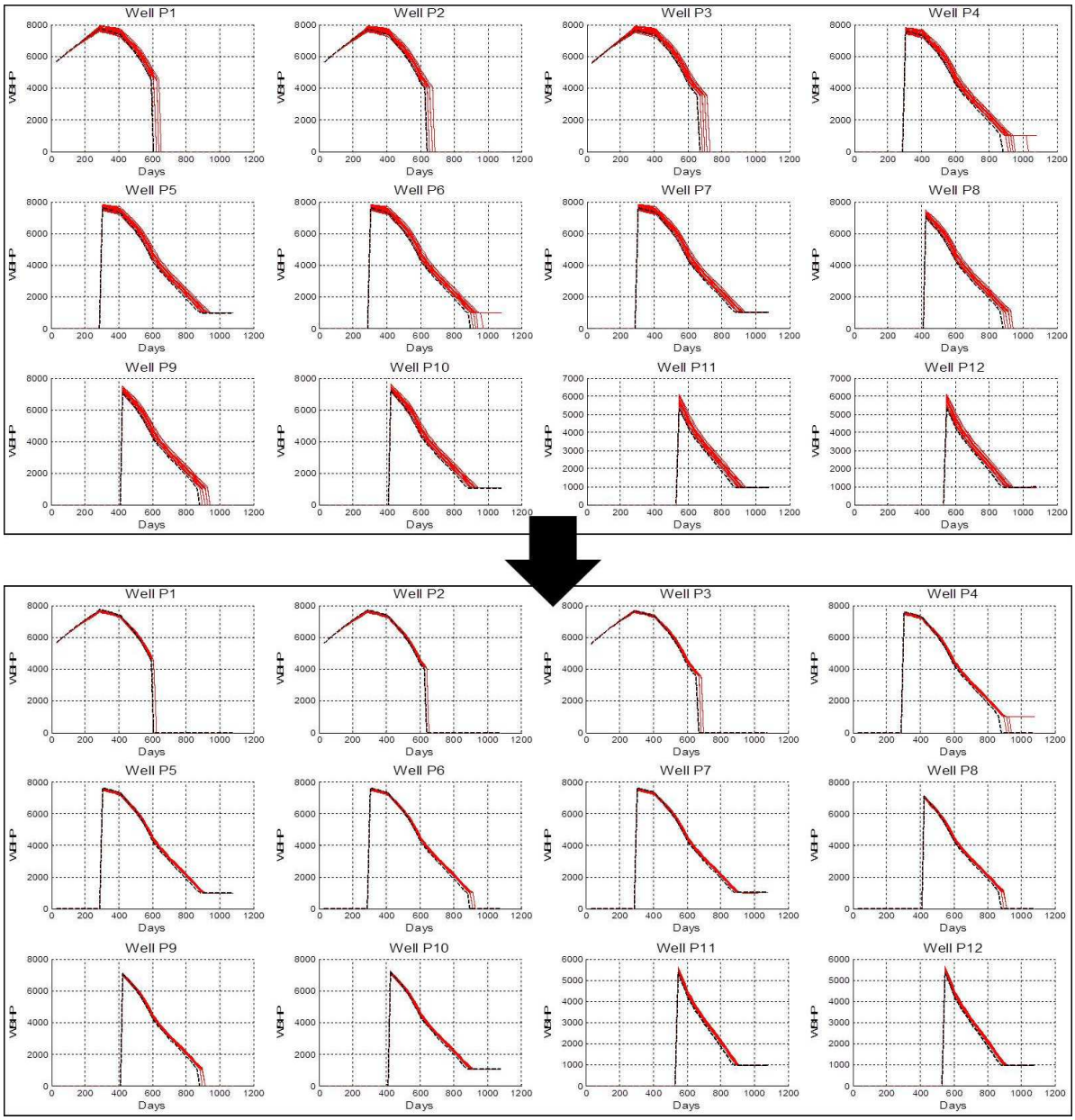

Figure 37 - Bottom hole pressure profiles convergence, form the first iteration at the last iteration (6), for each well individually during the 3 years production. Back dashed curve corresponds to the historic production data. The red thick line corresponds to the response of the 16 inverted models of the first and last iteration**.**

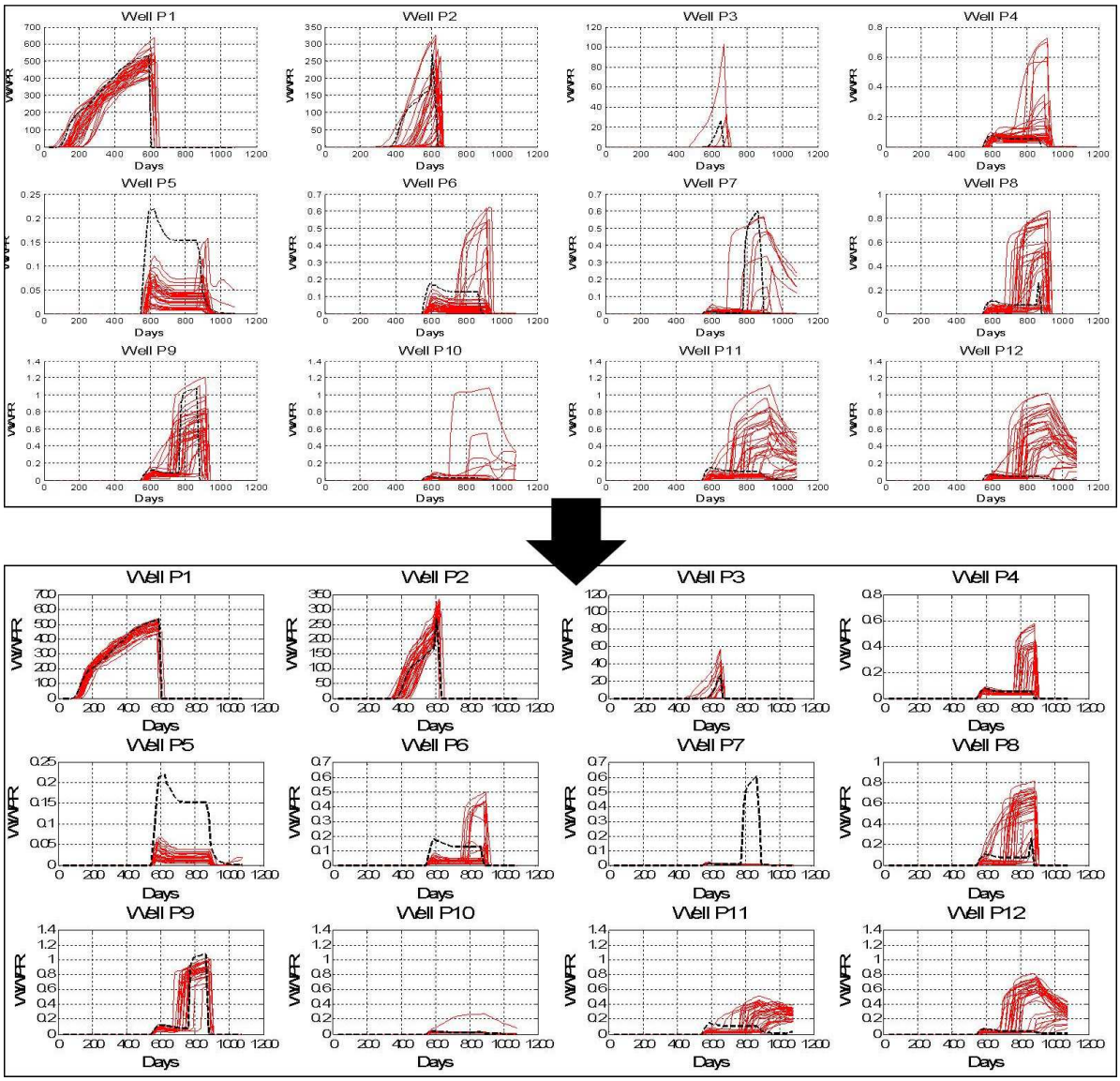

Figure 38 – Water production rate profiles convergence, form the first iteration at the last iteration (6), for each well individually during the 3 years production. Back dashed curve corresponds to the historic production data. The red thick line corresponds to the response of the 16 inverted models of the first and last iteration.

While the iterative procedure evolves from the first iteration to the next, the selection of the area of influence for each well individually uses as patchwork the higher correlation coefficients between the subsurface petrophysical property of interest and the production deviations. However, the correlation coefficients that may be high in areas with low feasibility of being influenced by a given well, are constraint in terms of concept of distances giving higher weight for values closer of each well (Different colours correspond to different areas of influence of each well (Figure 40)..

It is possible to visualize the evolution of area of influence from each well by the correlation coefficient, since only four wells were here illustrated (P2, P3, P5 and P10), and also notice that the correlation coefficient is higher from the first iteration to the last iteration (Figure 39). However, only the highest correlation coefficient from the twelve used wells is the one selected, which lead to the highest values obtained. As long as the iterative procedure evolves, it was not possible to ensure the convergence of the spatial continuity pattern of each area of influence, which reflects the rearrangement of the area of influence. The rearrangement of those areas was not as expected and it is open for further discussion in a future work.

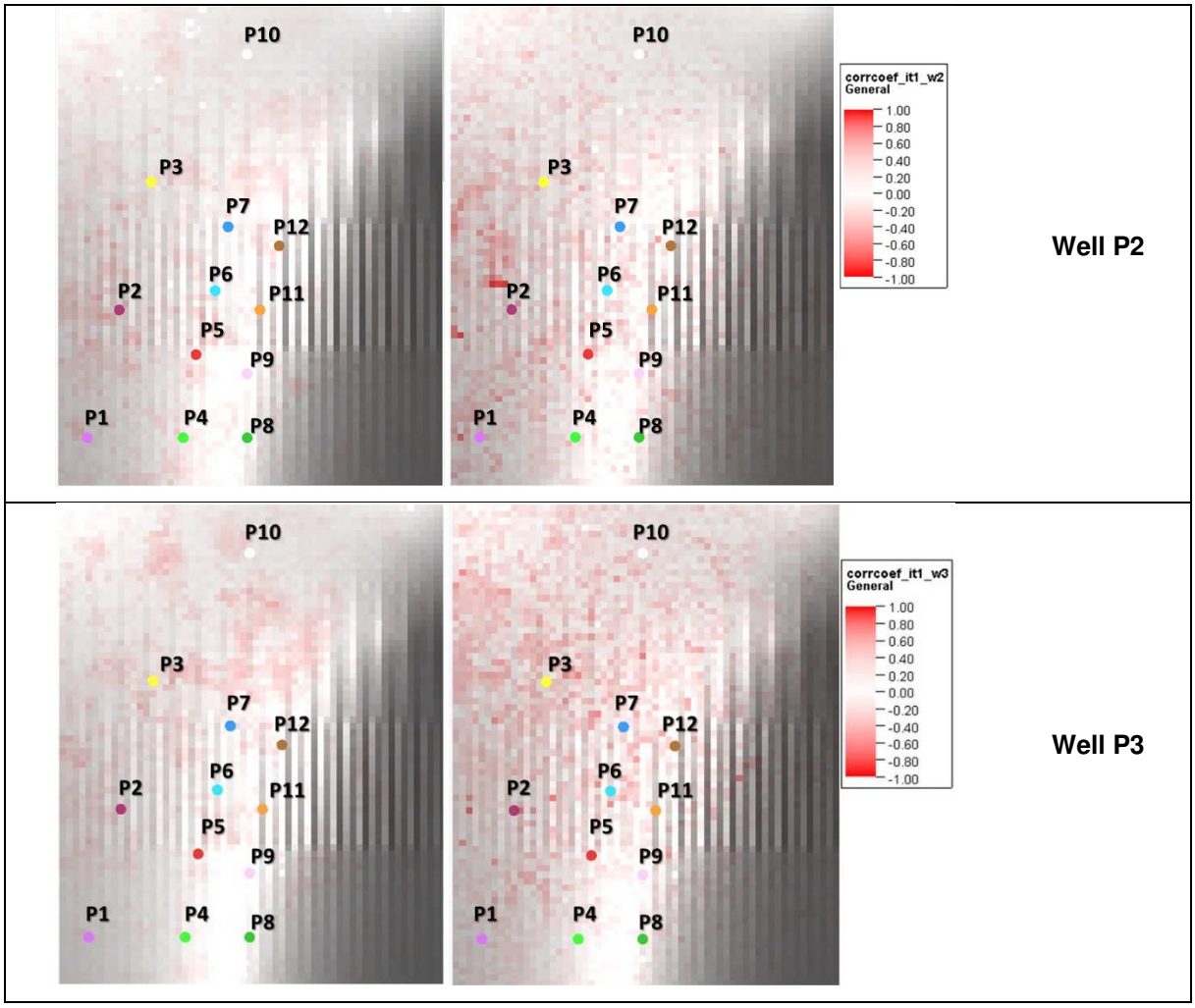

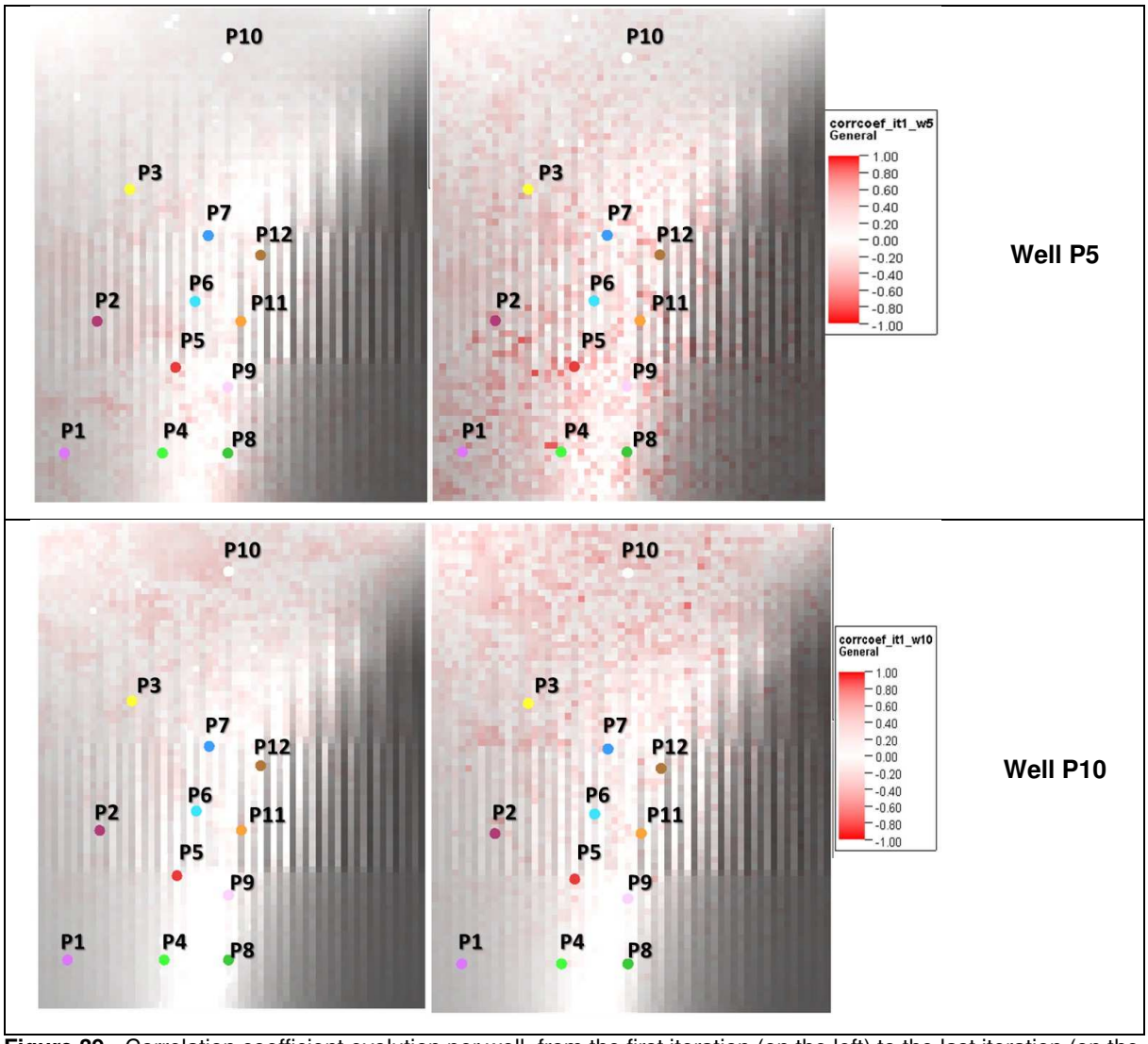

Figure 39 - Correlation coefficient evolution per well, from the first iteration (on the left) to the last iteration (on the right).

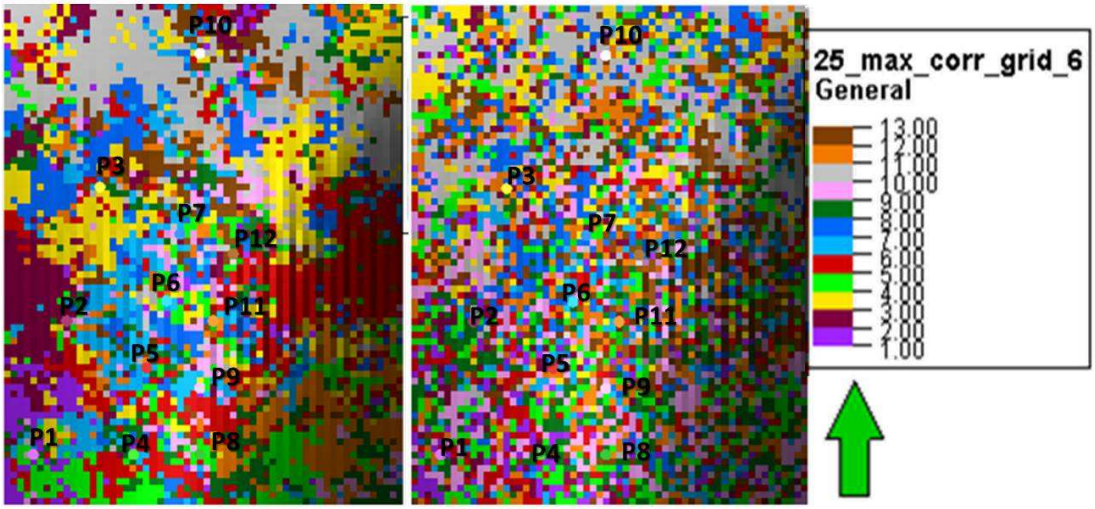

Figure 40 – Maximum correlation coefficients between permeability in each grid point and the deviations in each well at the end of (on the left) the first iteration and (on the right) the last iteration.

The impact of higher or less seismic influence within the iterative geostatistical procedure may be assesses through the convergence in terms of the objective function as the Figure 41 shows. In both cases the convergence is reached to a minimum value. When it is considered less seismic influence (red line) and consequently higher dynamic influence within the iterative procedure, the convergence is reached to a smaller value than in the higher seismic influence (blue line). Nevertheless the enhancement of the objective function convergence is reached as the iterative procedure evolves.

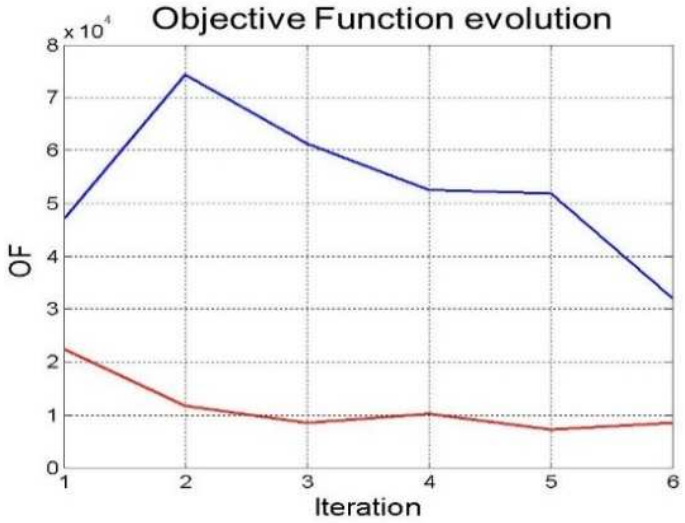

Figure 41 – Objective function evolution at the end of each iteration for the geostatistical history matching with seismic data integration: the red line with less influence of the seismic reflection and blue line with more influence of the dynamic data.

Another way to recognize how the model parameter space is explored by all the models computed during the iterative geostatistical procedure, is by plotting all the models of each well from the first and the last iteration. For this particular case study, the reduced space was created by retaining the first 2 eigenvalues that explain about 70% variance of the original model space. By plotting the dimension 1 versus dimension 2 it is easily recognizable that the iterative procedure is converging towards the real model response (Figure 42). It is also clear that with less seismic influence (on the right of the figure) the convergence among the 12 Wells is higher than (on the left of the figure) with higher seismic influence. Nevertheless, the Well 1, Well 2 and Well 3 shows also very good convergence, similar to the other case. This results are consistent as expected: while the seismic influence is higher it is more likely to have not accurate match towards the real ones as on the other hand.

The reproduction of the spatial continuity pattern in all the inverted petro-elastic models is ensured by using stochastic sequential simulation and co-simulation algorithms. Therefore, the spatial continuity pattern imposed by a variogram models estimated from the 12 wells (Figure 17) and the marginal and joint distributions (Figure 16 and Figure 18) are also reproduced in all the petro-elastic models simulated during the iterative inversion methodology (Figure 43, Figure 44 and Figure 45).

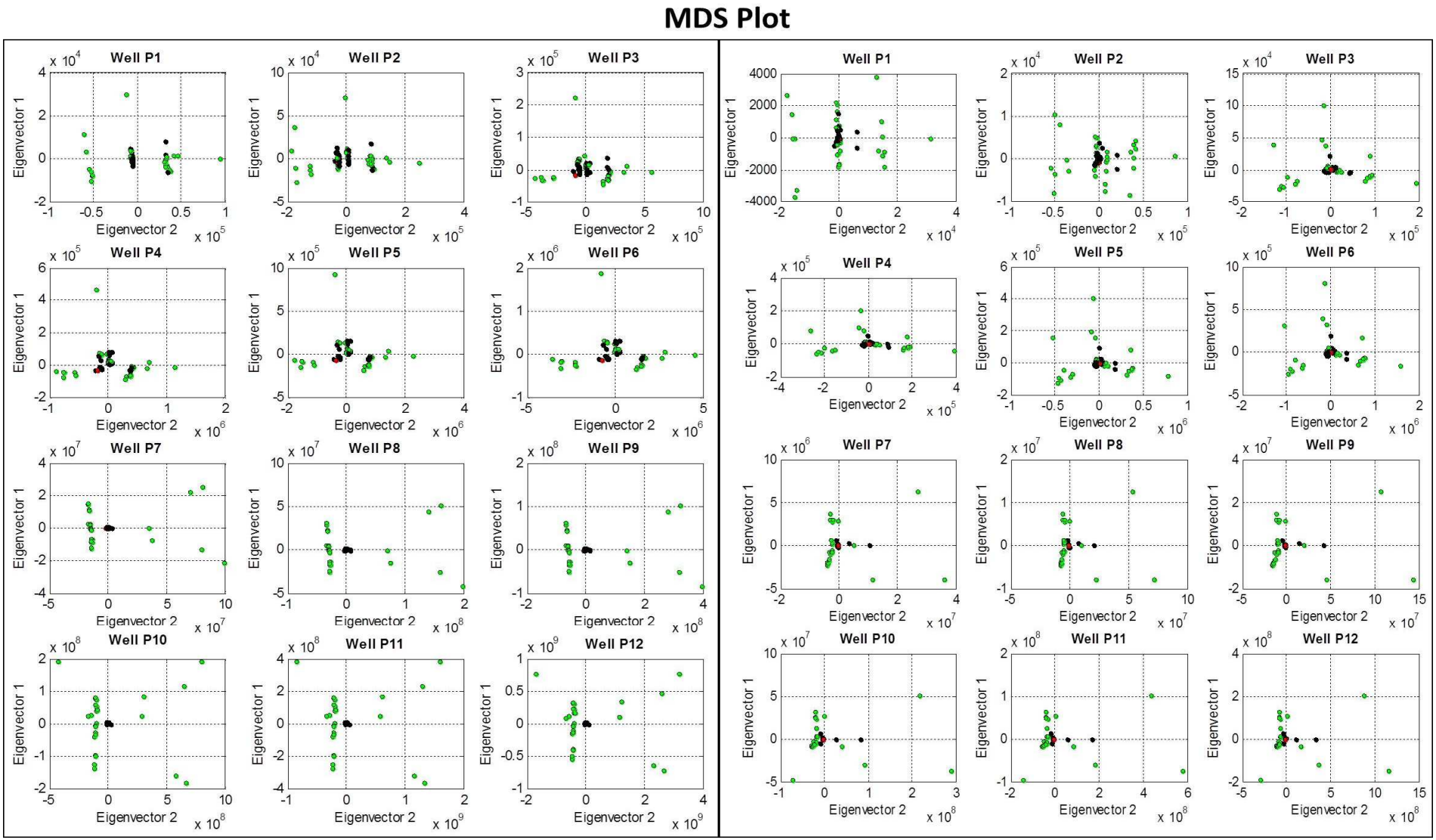

Figure 42 – MDS plots for all models produced in the first iteration (green circles) and the last iteration (black circles) from the 12 wells used in the iterative geostatistical procedure: (on the left) the case were it is considered higher seismic influence and (on the right) the case were it is considered less seismic influence. The true models are represented by the red circle

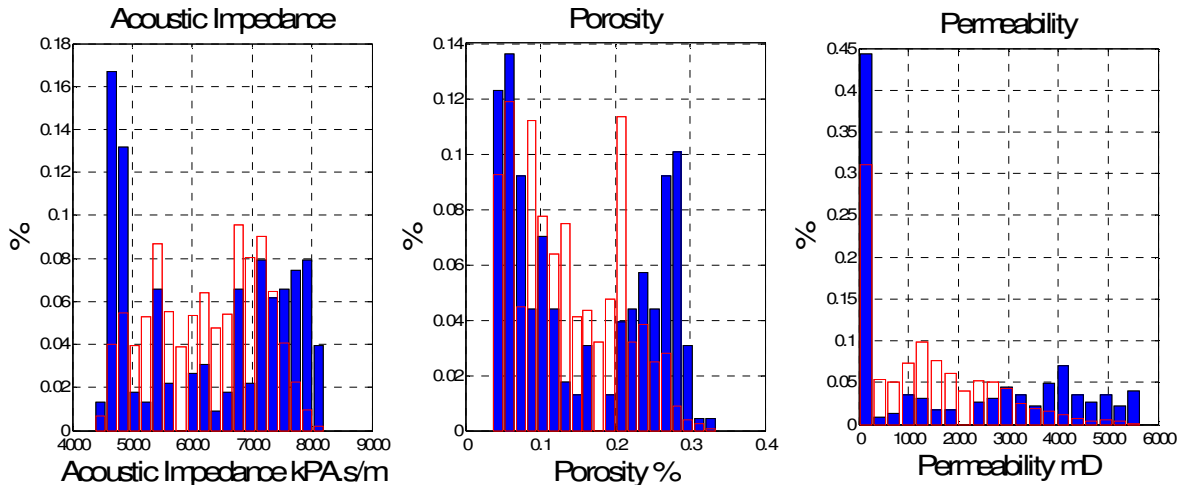

Figure 43 - Comparison between the marginal distributions of acoustic impedance, porosity and permeability estimated from the well-log data (in red) and those retrieved from the last elastic inverted model from the last iteration (blue filled bars).

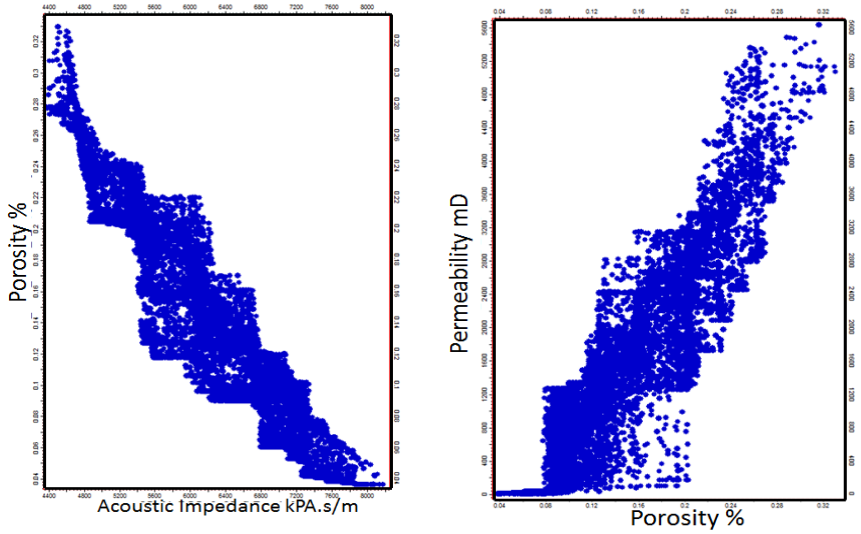

Figure 44 - Joint distributions estimated from the last elastic inverted model from the last iteration: (on the left) acoustic impedance versus porosity and (on the right) porosity versus permeability. They reproduce the joint distributions estimated from the well-log data.

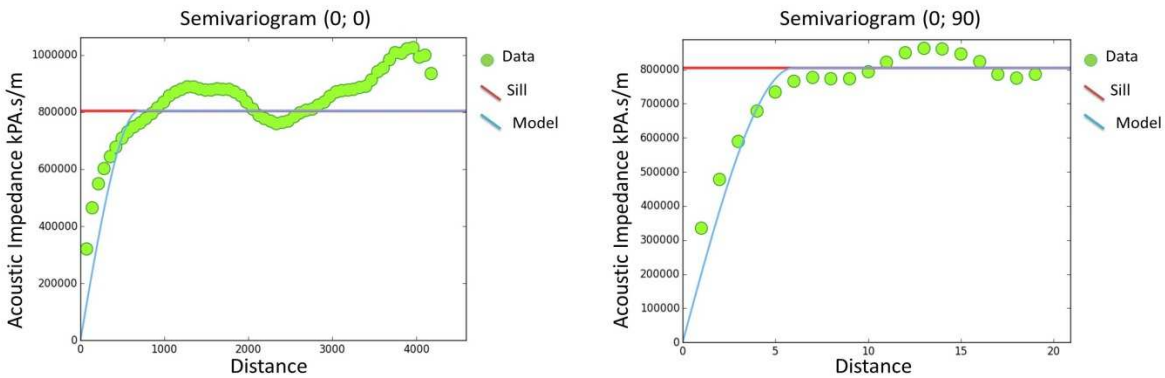

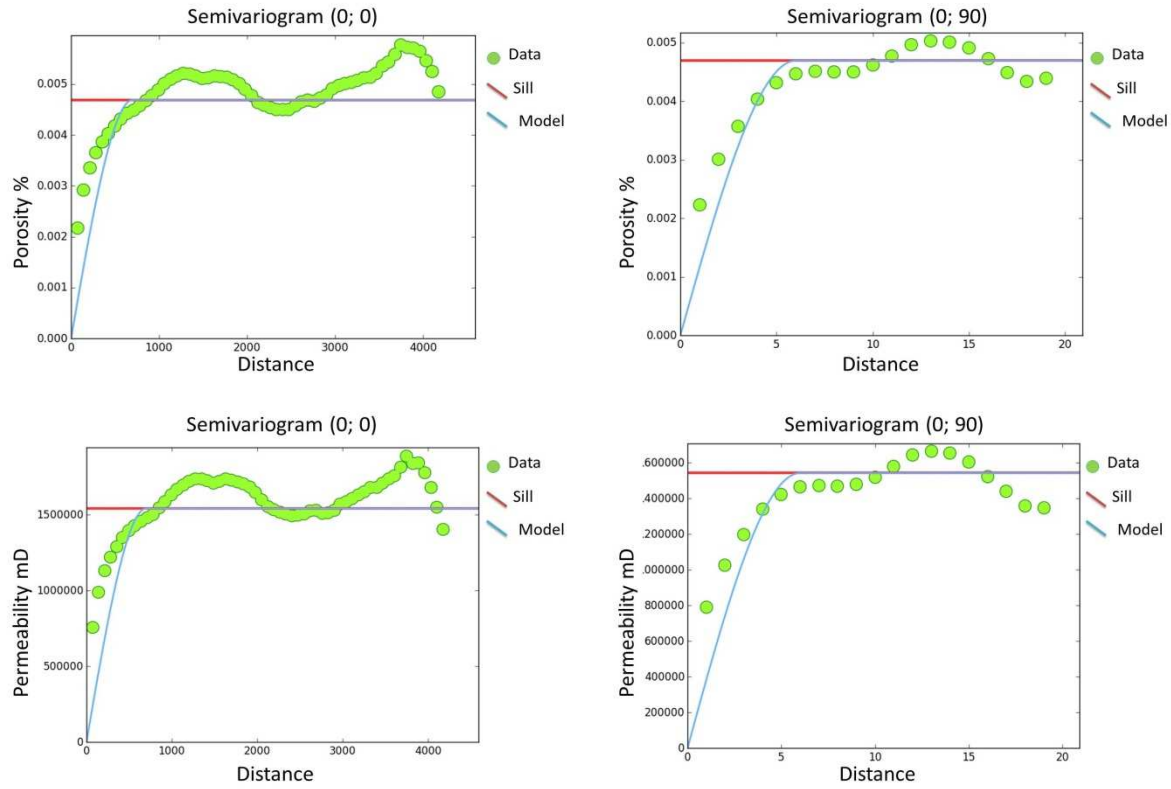

Figure 45 - Experimental (green circles) and modeled variograms (blue line) for the omnidirectional (on the left) and vertical directions (on the right) for: (from top to bottom) acoustic impedance, porosity and permeability. The variograms were computed over one grid model of the sixth iteration (compare with Figure 17).

4.3. Discussion

In general, the implementation of the geostatistical history matching with seismic data integration is very promising since the results from different areas of influence are consistent with the real petro-elastic models. In the inverted petro-elastic model, the major patterns are reproduce even though it is difficult to represent reservoir models with non-stationary patterns associated with meandering channels. The iterative optimization assures simultaneously the match between observed seismic and historic production data.

The methodology introduced herein ensures the reproduction of the joint distributions between acoustic impedance versus porosity and porosity versus permeability, and the corresponding marginal distributions for each petro-elastic property individually. It is very important to reproduce the relationships between the petro-elastic properties of interest since they directly refer to the subsurface geologic characteristics. As a geostatistical methodology and constrained by well-log data all the inverted models honour the values of the well-log data at its location. The spatial continuity models, as inferred by a variogram model estimated from the available wells and imposed by the DSS and co-DSS algorithms, are reproduced in all the inverted petro-elastic models generated during the iterative procedure.

The application example shown in this section studies two different criteria to define the areas of influence of each well: geometrical and according to correlation coefficients between permeability in

each grid point and the deviation in each well. While the geometric criteria takes only into account the match towards the real historic production and seismic data within the areas of influence from each well and outside those areas are constrain to the match towards the real seismic data, by defining the area of well influence according to correlation coefficients it is possible to constrain all reservoir extent to the match towards both inverse problems at the same.

By integrating seismic reflection data within the history matching procedure we are able to reproduce the real subsurface patterns that are able to match simultaneously the observed seismic reflection and production data. The inclusion of seismic reflection data is able to constrain the inference of the petro-elastic properties far from the well locations and enable the geostatistical seismic inversion to reproduce complex and non-stationary patterns like the meandering channels presented in this work,

The history matching procedure towards the historic production data when considering a lower weight on the dynamic part of the multi-objective function and consequently a higher weight on the seismic reflection data reproduces higher misfit than on the contrary, however, as the iterative procedure continues the convergence is ensured as shown in Figure 41. From the interpretation of the MDS plots for both examples for each well (Figure 42) it is clear that the inverted petro-elastic models start to converge towards the real ones, which directly refers to the degree of uncertainty associated with, as well as the uncertainty space exploration from iteration to iteration.

Nevertheless, besides the success of the convergence of both inverse problems, the second criteria does not reproduce the spatial continuity of the areas of influence near the wells location as expected when it was considered the imposed concept of distances.

Chapter 5. Conclusions and Future Work

This thesis presents a new methodology of geostatistical history matching with seismic data integration, which allows us to build high resolution petro-elastic models conditioned simultaneously to the known data: well-log data, seismic data and historical production data; where while the history match towards the historic production data is performed the inverted petro-elastic models starts to converge to the real ones.

The main goal of this study was to provide a new workflow for geostatistical history matching procedure by integrating the seismic reflection data in order to improve the spatial continuity of the inverted petro-elastic models in all reservoir extent, i.e. to tackle the geological inconsistency in history matching techniques by enhance the spatial continuity of the properties (acoustic impedance, porosity and permeability) not only in areas near the wells location but particularly at location far from the wells where the constraining data is fewer. It also allows to, in early stages, the assessment of the spatial uncertainty of all reservoir extent. The problem associated with the evaluation of the static models through their dynamic responses is the relation between the petrophysical parameters and the associated dynamic responses which are highly non-linear and spatially non-stationary. The meandering channels have complex non-stationary structures and the fluid flow has preferential paths, the sand channels, which is very demanding and requires advanced techniques to solve the problems related with the non-stationary modelling.

The presented methodology demonstrated to have high potential, since the proposed algorithms are able to solve both inverse problems, history matching and seismic inversion at the same, providing more reliable petrophysical models. The proposed methodology consists in a genetic algorithm which perform at the same the seismic inversion and the history matching using as input the porosity and permeability models conditioned to the seismic in order to obtain more realistic shapes of the channels with faster convergence of the dynamic responses. This way, this iterative process by taking into account the correlation coefficients between permeability in each grid point and the deviations in each well allows to tackle the problem of non-stationarity resulting in accurate descriptions of complex continuous and connected structures. Therefore in order to solve the highly non-linear and spatially non-stationary problem associated with the evaluation of the static models through their dynamic responses.

The results of this study ensure the reproduction of the joint distributions between acoustic impedance versus porosity and porosity versus permeability, and the corresponding marginal distributions for each petro-elastic property individually. It is very important to reproduce the relationships between the petro-elastic properties of interest since they directly refer to the subsurface geologic characteristics. As a geostatistical methodology and constrained by well-log data all the inverted models honour the values of the well-log data at its location. The spatial continuity models, as retrieved by a variogram model estimated from the available wells, are also reproduced in all the inverted petro-elastic models generated during the iterative procedure.

With the implementation of this methodology it possible to simulate models with high resolution conditioned in all reservoir extent to both inverse problems, which translates in a solution for the history matching techniques as well as the integration within the same framework of the inversion of acoustic impedance, porosity and permeability models conditioned to the well-log data, seismic reflection and dynamic data.

In general, this workflow is very promising since the results were very consistent with the reference model. Besides the encouraging results, this workflow may be improved, essentially in terms of the areas of influence definition since it only takes into account the mean deviations of each well and the correlation with the petrophysical property. Thus, by considering an objective function and being more precise in the correlation coefficients calculation, it might be possible to obtain areas of influence with more realistic spatial continuity. However, it will be challenging to see this methodology applied to a real reservoir with those complex structures as the meandering channels. The definition of the well influence area may for example be defined by the evaluation of the connectivity of the channels since the reservoir is dynamic the fluids have preferential fluid paths and in non-stationary geological features such as the thickness, width and shape of deltaic reservoirs a small change can have huge impact on production forecast and match. Therefore, the use of stream-lines may be an indicator for the well influence area definition.

The seismic reflection data used as real seismic data within the iterative procedure of this algorithm was acquired one time, in a certain moment previous the production starts, so we may have some inconsistency problems regarding the inverted petro-elastic models because sparsely along the field, namely near the wells, the oil is no longer present but water. This gives different Ip velocities changing all the initial characterization of the reservoir. However this is more evident at each well location were the dynamic data is measured. Thus, the integration of 4D seismic could be enhance algorithm in order to retrieve better reservoir models.

References

Azevedo, Leonardo (2013) “Geostatistical methods for integrating seismic reflection data into subsurface Earth models”, PhD Thesis, Instituto Superior Técnico, Portugal

Bosch, M., Mukerji, T, González, E. (2010) “Seismic inversion for reservoir properties combining statistical rock physics and geostatistics: A review” *Geophysics Vol. 75*, ResearchGate

Caers, Jeff (2005) “Petroleum Geostatistics” SPE

Caers, Jef (2011) “Modelling Uncertainty in the Earth Sciences” UK: Wiley-Blackwell

Caeiro, Maria Helena (2014) “Optimised history matching using non-stationary geostatistical modelling”, PhD Thesis, Instituto Superior Técnico, Portugal

Carneiro, João (2010) “Modelo de Optimização para o Processo de *History Matching* de Reservatórios Petrolíferos”

Chen, W., Gavalas, G., Wasseman, M. (1973) “A new algorithm for automatic history matching” SPE 4627, SPE-AIME 48th Annual Fall Meeting, Las Vegas, U.S.A., September 30 – October 3

Christie, M., Eydinov, D., Demyanov, V. and Talbot, J. (2013) “Use of multi-objective algorithms in history matching of a real field” SPE Reservoir Simulation Symposium.

Deutsch, C. and A.G. Journel (1998) “GSLIB: Geostatistical Software Library and User’s Guide.” Oxford University Press

Goovaerts, Pierre (1997) “Geostatistics for Natural Resources and Evaluation.” Oxford University Press

Hajizadeh, Y., Christie, M., Demyanov, V. (2010) “History Matching with Differential Evolution Approach; a Look at New Search Strategies” SPE EUROPE/EAGE Annual Conference and Exhibition. Barcelona, Spain. SPE – 130253

Hoffman, Todd (2005) “Geologically consistent history matching while perturbing facies” PhD Thesis, Institute of Petroleum Engineering, Herriot Watt University, UK

Horta, Ana, and Soares, Amilcar (2010) “Direct Sequential Co-Simulation with Joint Probability Distributions.” Mathematical Geosciences 42: 269-292. Doi:10.1007/s11004-010-9265-x.

Jacquard, P. (1965) “Permeability distribution from field pressure data” SPE Journal, 5:281-294

Kruger, W. D. (1960) “Determining areal permeability distribution by calculations” SPE 1580, 35th Annual Fall Meeting of SPE, Denver, U.S.A., 2-5 October

Mata-Lima, Herlander (2008) “Reservoir characterization with iterative direct sequential co-simulation: integrating fluid dynamic data into stochastic model” Journal of Petroleum Science and Engineering. 62, 59-72.

Ouenes, A., Bhagavan, S., Bunge, P.H., and Travis B.J. (1994) “Application of simulated annealing and other global optimization methods to reservoir description: Myths and realities. In SPE 69th Annual Conference and Exhibition, New Orleans, LA, pages 547-561. SPE paper number 28415.

Rwechungura, R., Dadashpour, M., Kleppe, J. (2011) “Advanced History Matching Techniques Reviewed” SPE – 142497

Soares, Amílcar (2001) “Direct Sequential Simulation and Cosimulation” Mathematical Geology, Vol. 33, No. 8.

Soares, Amílcar (2006) “Geostatística Para as Ciências Da Terra e Do Ambiente” IST Press.

Soares, Amilcar, Diet, J.D. and Guerreiro, Luis (2007) “Stochastic Inversion with a Global Perturbation Method”, EAGE

Tarantola, Albert (2005) “Inverse Problem Theory” SIAM

Tyler, K., Svanes, T., Omdal, S. (1993) “Faster history matching and uncertainty in predicted production profiles with stochastic modelling” SPE 26420, 68th Annual Technical Conference and Exhibition of the SPE, Houston, Texas, 3-6 October

Wang, Y. and Kovscek, R., (2003) “Integrating production history into reservoir models using streamline-based time-of-flight ranking”, Petroleum Geoscience, Vol. 9 Iss. 2, pp 163-174